

DEC 1 1964



*Technical Note*

*No. 219*

---

# RADIO PATH LENGTH STABILITY OF GROUND-TO-GROUND MICROWAVE LINKS

M. C. THOMPSON, Jr., and H. B. JANES



---

U. S. DEPARTMENT OF COMMERCE  
NATIONAL BUREAU OF STANDARDS

## THE NATIONAL BUREAU OF STANDARDS

The National Bureau of Standards is a principal focal point in the Federal Government for assuring maximum application of the physical and engineering sciences to the advancement of technology in industry and commerce. Its responsibilities include development and maintenance of the national standards of measurement, and the provisions of means for making measurements consistent with those standards; determination of physical constants and properties of materials; development of methods for testing materials, mechanisms, and structures, and making such tests as may be necessary, particularly for government agencies; cooperation in the establishment of standard practices for incorporation in codes and specifications; advisory service to government agencies on scientific and technical problems; invention and development of devices to serve special needs of the Government; assistance to industry, business, and consumers in the development and acceptance of commercial standards and simplified trade practice recommendations; administration of programs in cooperation with United States business groups and standards organizations for the development of international standards of practice; and maintenance of a clearinghouse for the collection and dissemination of scientific, technical, and engineering information. The scope of the Bureau's activities is suggested in the following listing of its four Institutes and their organizational units.

**Institute for Basic Standards.** Electricity. Metrology. Heat. Radiation Physics. Mechanics. Applied Mathematics. Atomic Physics. Physical Chemistry. Laboratory Astrophysics.\* Radio Standards Laboratory: Radio Standards Physics; Radio Standards Engineering.\*\* Office of Standard Reference Data.

**Institute for Materials Research.** Analytical Chemistry. Polymers. Metallurgy. Inorganic Materials. Reactor Radiations. Cryogenics.\*\* Office of Standard Reference Materials.

**Central Radio Propagation Laboratory.\*\*** Ionosphere Research and Propagation. Troposphere and Space Telecommunications. Radio Systems. Upper Atmosphere and Space Physics.

**Institute for Applied Technology.** Textiles and Apparel Technology Center. Building Research. Industrial Equipment. Information Technology. Performance Test Development. Instrumentation. Transport Systems. Office of Technical Services. Office of Weights and Measures. Office of Engineering Standards. Office of Industrial Services.

---

\* NBS Group, Joint Institute for Laboratory Astrophysics at the University of Colorado.

\*\* Located at Boulder, Colorado.

NATIONAL BUREAU OF STANDARDS

*Technical Note 219*

Issued November 15, 1964

**RADIO PATH LENGTH STABILITY OF  
GROUND-TO-GROUND MICROWAVE LINKS**

M. C. Thompson, Jr., and H. B. Janes  
Central Radio Propagation Laboratory  
National Bureau of Standards  
Boulder, Colorado

NBS Technical Notes are designed to supplement the Bureau's regular publications program. They provide a means for making available scientific data that are of transient or limited interest. Technical Notes may be listed or referred to in the open literature.



## Table of Contents

<u>Section</u>	<u>Page No.</u>
1. Introduction . . . . .	1
2. Data Analysis . . . . .	4
2.1. General . . . . .	4
2.2. Long-Term Variations. . . . .	4
2.3. Power Spectrum Analysis . . . . .	5
2.4. Correlation of Spectral Density Variations with Meteorological Data . . . . .	8
2.5. Signal Amplitude Variations. . . . .	9
2.6. Comparison of 100 Mc/s and 9400 Mc/s Data . . . . .	10
2.7. Path Length Difference Data . . . . .	11
3. Conclusions . . . . .	13
4. Appendix . . . . .	15
4.1. Tower Motion Study. . . . .	15
5. References . . . . .	17
Figures 1 through 50 . . . . .	19 through 68



# Radio Path Length Stability of Ground-to-Ground Microwave Links

M. C. Thompson, Jr., and H. B. Janes

The Lower Atmosphere Physics Section of the National Bureau of Standards, Troposphere and Space Telecommunications Division, conducted a series of eight field experiments in 1958 and 1959 to study the variation in the apparent path length of ground-to-ground microwave links (i. e., the variations in phase of 9400 Mc/s signals) and the corresponding variations in radio refractive index and other atmospheric parameters measured at the path terminals. This report summarizes the results obtained on paths in Colorado and Florida. It also includes an analysis of long-term variations in the apparent path length and associated variables recorded during each experiment, and a power spectrum analysis of short-term variations in apparent path length and refractivity.

## 1. Introduction

During the period from September 1958 to November 1959 the Lower Atmosphere Physics Section of the National Bureau of Standards conducted a series of eight experiments to study the time variations in the electrical lengths of nearly-horizontal, ground-to-ground, line-of-sight radio links.<sup>1</sup> These were conducted under a variety of environmental conditions such as might be encountered in the operation of electronic guidance, tracking, and direction-finding systems. The

---

<sup>1</sup>This work was sponsored, in part, by the U. S. Air Force Ballistic Missile Division under contract number AF 04(647) - 134.

purpose of the experiments was to study the statistical properties of the apparent path length variations and their dependence on various meteorological parameters.

The method used for measuring the apparent path length fluctuations is basically a phase comparison technique which has been described previously [Thompson and Vetter, 1958]. The most important atmospheric parameter in this study is the radio refractivity<sup>2</sup>, which was measured in two ways. The long-term variations were obtained from observations of temperature, pressure, and relative humidity. The short-term variations were recorded by the use of a microwave refractometer. Standard meteorological techniques were used to record atmospheric pressure, temperature, relative humidity, wind velocity, and (in some cases) incident solar radiation (insolation) at one or both path terminals.

The first of the experiments (referred to hereafter as "runs") was made over a 15.2 km path near Boulder, Colorado, during a 40 hour period in September 1958. A map and terrain profile of this path are shown in figures 1 and 2. The principal objectives were to study path length variations at 9400 Mc/s over a path having little or no ground reflection, using both horizontal and vertical polarization. The second run, in October, was a continuation of the same type of measurements made in September, but narrower-beam antennas were used and the length of the run was extended to five days to more adequately study day-to-day variations.

---

<sup>2</sup>The radio refractivity, N, is defined by

$$N = (n - 1) \times 10^6,$$

where n is the radio refractive index.

The third run was made at 9400 Mc/s in February 1959, using a 713 m path near Boulder (figures 3 and 4). Simultaneous path length (phase) variation recordings were made on two paths having one terminal in common and the other terminals separated vertically, one near maximum and the other near minimum of the height-gain pattern. The purpose of this run was to study the effect of ground reflections on phase stability.

The fourth run was made over a 3.2 km path near Boulder in June (figures 5 and 6), again using a 9400 Mc/s signal. This run supplied information on path length stability over a path longer than that used in February, but one having the same flat terrain and low antenna heights, thereby ensuring the existence of ground reflections.

The fifth run, in July, used the same 15.2 km path used in the first two runs. Simultaneous 9400 Mc/s and 100 Mc/s path length stability recordings were made to test the feasibility of using the lower frequency and also to provide a comparison of stability recordings made under different ground reflection conditions.

The remaining runs were made on or near the Air Force Missile Test Center at Cape Canaveral\*, Florida, to gather data under the same climatic conditions under which actual systems are operated. The sixth run was made at 9400 Mc/s over a 7.7 km path over flat terrain and at approximately grazing incidence to foliage on the path (figures 7 and 8). The seventh run was made over the same path but with path length variations observed simultaneously at vertically spaced antennas at one of the terminals; one antenna placed to provide a path slightly above, and the other slightly below, grazing incidence (figure 8).

The last run was made over a 17.1 km path extending from Cape Canaveral to a point north of Cocoa, Florida (figures 9 and 10). The purpose here was to study the effect of increased path length. Again

---

\* This work was done before the name was changed to Cape Kennedy.

vertically spaced antennas were used at one terminal, one providing a path at approximately grazing incidence with the foliage, and the other below grazing incidence.

## 2. Data Analysis

### 2.1. General

In general, the data output from each run consisted of continuous recordings of apparent path length variations, radio refractive index at one path terminal using a microwave refractometer, insolation, and horizontal wind velocity at both terminals. In addition, wet and dry bulb temperatures and barometric pressure readings were taken at half-hour intervals. During the last two runs, signal amplitude variations were also recorded continuously.

The path length and refractometer data were divided into two recording pass-bands: a "low-pass" record covering the spectral region from 0 to about 1 c/s, and a "band-pass" record extending from 0.03 to 10 c/s. Examples of path length and refractivity data are shown in figures 11 through 14.

The band-pass data were subjected to an analog power spectrum analysis to show the shape of the path length and refractivity spectra in the region from 0.1 to 20 c/s and also to indicate the variation of spectral density with time and certain atmospheric characteristics.

### 2.2. Long-Term Variations

The long-term variations in phase, refractivity, and meteorological data are shown in figures 15 through 22. To obtain the graphs of phase and wind speed and direction, the continuous chart records were read at half-hour intervals. The effective averaging time for these variables is estimated to be several seconds except for very low wind speeds, for which the averaging time may become much larger.

Temperature, humidity, and pressure graphs are plotted from the observations of the wet-and-dry bulb thermometers and the barometer, made at half-hourly intervals. In each of these readings the averaging time is estimated to be about 10 seconds. The refractivity curves are calculated from these meteorological observations.

It should be noted that in the case of phase and refractometer recordings no absolute calibrations were available. Thus the data permit only examination of the relative variations in these parameters. The data calculated from the barometer and psychrometer readings provide the absolute measure of refractivity shown in the graphs.

These graphs illustrate the wide variety of path length variations that can be observed on any path lying at least partially in the lower troposphere. For example, path length changes of as much as 30 parts per million occurred during a 24-hour period (figures 15 and 22). These changes generally occur most rapidly near sunrise and sunset. On occasion, excursions of 5 ppm occurred over a period of 10 minutes. Conversely, during the night it was not uncommon for the phase to remain within a few parts in 10 million for periods of hours (figure 13).

The path length variations are in most cases well correlated with refractivity data taken at the path terminals. Although the temperature and relative humidity usually exhibited a noticeable diurnal cycle, the path length data, in general, were dominated by longer-term variations or "trends" caused by gradually changing weather conditions, and a diurnal cycle is often not discernible.

### 2.3. Power Spectrum Analysis

The short-term fluctuations in apparent path length and refractivity were subjected to a power spectrum analysis, which indicates how much of the variance (mean of the squared deviations from the sample mean value) is contributed by fluctuations falling into each of

several narrow bands of fluctuation frequencies. As used here, "short-term variations" refers to the relatively small and rapid deviations about the larger long-term trends. The purpose of the spectrum analysis was to study the behavior of the spectral density (i. e., variance per unit bandwidth) as a function of time and other parameters.

During runs 1 and 2 (September and October 1958), all of the recordings were made on paper charts. The power spectra for these runs were obtained by digitizing the chart record manually and computing the Fourier transform of the autocovariance function. The computing method used is essentially that suggested by Blackman and Tukey [1958]. This analysis has been described in detail previously [Thompson, Janes, and Kirkpatrick, 1960; Thompson and Janes, 1959].

In runs 3 through 8, all band-pass data were recorded on magnetic tape, which permitted the use of analog spectrum analysis techniques. In this case, the power spectrum analysis consisted essentially of passing a voltage proportional to the variable through a very narrow-band filter and recording the mean squared output as a function of time for each of several spectral frequencies. A time plot of spectral density at each frequency was then obtained by dividing the mean squared filter output by the filter bandwidth. The tape was fed through the analyzer at a speed 100 times greater than that used in recording. This was done to reconcile the difference between the frequency ranges of the recording and analyzing equipment. For example, the 2 c/s filter bandwidth and frequency range of 3 to 2000 c/s used in the analyses correspond to a bandwidth of 0.02 c/s and a frequency range of 0.03 to 20 c/s in recording time. An averaging circuit having a time constant of 4 seconds (6-2/3 minutes in recording time) was used for averaging the squared filter output in all cases except the 100 Mc/s data for July 1959. In the

latter case, a 1-second time constant was used for the lower spectral frequencies. One disadvantage of this method is that discontinuities of any kind in the tape data cause large transients in the analyzer output. In scaling the latter for the half-hourly values of spectral density shown in this report, considerable care was exercised to avoid the effects of discontinuities.

The results of the analog power spectrum analysis of the 9400 Mc/s path length and refractivity data are summarized in figures 23 through 26. They consist of families of spectral-density-versus-time curves with frequency as the parameter. In general, the power spectra show a diurnal cycle with increased spectral density during the daylight hours. In the Florida data this night-to-day increase was on the order of 10 to 1 in apparent path length, and even larger in refractivity (figure 25). The Colorado data showed a smaller diurnal variation.

Figure 27 shows the median values of the spectral densities of refractivity (N) and path length plotted as a function of frequency and divided into daytime (7:00 a.m. to 6:00 p.m.) and nighttime data (6:30 p.m. to 6:30 a.m.). Similar curves are shown in figure 28 for run 4 (June 1959). These curves serve to illustrate the slopes of the various spectra and the size of the day-to-night changes in spectral level. It should be noted that there is little or no systematic change in slope in going from day to night, or from Colorado to Florida.

It would appear that the path length spectral density is significantly higher in Florida than in Colorado. However, it was found that the particular analog spectrum analysis equipment used here could yield results that in repeated trials differed in absolute level (i. e., spectral density) by as much as a factor of 2. However, the relative accuracy of spectral estimates at the various frequencies within a given run was much better (within about 20 %). Consequently, the

shapes of the median spectra are considerably more reliable than their absolute levels. This should be borne in mind in comparing the spectra obtained in different runs of this series.

#### 2.4. Correlation of Spectral Density Variations With Meteorological Data

Figures 29 through 34, inclusive, show the spectral density curves at 1 or 3 c/s taken from the previous graphs compared with the corresponding wind speed, temperature, refractivity, and insolation. The question of correlation between spectral density and the meteorological variables is a difficult one to answer quantitatively. Although each of these variables was sampled at the rate of two readings per hour, the effective "pass-bands" of their respective measuring systems are not necessarily similar. In particular, the smoothness of the spectral density curves was determined arbitrarily by the choice of the time constant used in the wave analyzer (6-2/3 minutes in this case).

However, it appears that of the variables selected for comparison, the wind speed and temperature are most likely to be significantly correlated with the apparent path length and refractivity spectral densities. They all show a similar diurnal cycle with generally higher spectral levels, temperatures, and wind speeds during the daytime. On the other hand, it is not hard to find examples of correlation on an hour-to-hour basis between spectral density and wind speed. In an effort to describe these apparent correlations quantitatively, the spectrum of each of the variables was separated into two parts: the lower frequency variations were isolated by computing a 6.5-hour running average of the half-hourly values, while the higher frequency variations are simply the deviations of the original data about this running average. The correlation coefficients of both the low-frequency

and high-frequency variations of spectral density with wind speed and temperature were computed for the July, Colorado, run and the September, Florida, run. Figures 35 through 38 summarize the results.

During the July run in Colorado, the long-term wind speed lagged (i. e., occurred after) the temperature variations by about three hours. Hence, the correlation curves of wind and temperature versus spectral density are displaced relative to each other by that amount. It is interesting to note that the long-term path length spectra correlate best with average end-point wind speed with very little lag, while the refractivity spectra correlate best with temperature with no lag. This would indicate that the path length spectral density lagged the refractivity spectral density by roughly three hours.

## 2.5. Signal Amplitude Variations

During the runs of October 10-12 and October 30 - November 3, 1959, in Florida, amplitude recordings were made on both the upper and lower paths. These results are summarized in figures 39 and 40, which show plots of samples read at 30-minute intervals. In both runs and on both paths, regions of rapidly changing field strength were observed. Between 1300 and 1400 on October 11, the signal received at the upper antenna increased by nearly 12 db, while that at the lower antenna increased by almost 9 db. Between 0700 and 0800 of the same day, the upper path signal increased by 6 db, while the lower was increasing by 12 db. During the early part of October 12, both signals were some 10 or more db lower for several hours than their average values and did not recover until after sunrise.

This is believed due to changes in the multipath resulting from slight changes in the refractivity gradient near the ground. In these paths, the surface vegetation and terrain combined to make it very difficult to determine the effective antenna height. However, the

limited height-gain data which could be obtained indicated that there was a significant ground-reflected component. The observed range of signal amplitudes of about 20 db would require (on this basis) a reflection coefficient of about 0.9, which is not unreasonable considering the very low angle of incidence (practically grazing). Since the paths (both direct and ground-reflected) were about  $2 \times 10^5 \lambda$  long, a change in average refractivity of 2.5 N-units along the path would produce a change of  $180^\circ$  in the phase of the signal arriving over that path. Thus, a change in signal strength of 20 db would imply, for this path, a change in the refractivity difference of the order of a few N-units over the vertical separation of about 15-feet. In the area involved, it is felt that this is not unreasonable in the region immediately above the terrain.

#### 2.6. Comparison of 100 Mc/s and 9400 Mc/s Data

Multipath is believed responsible for the major differences noted in the apparent path length variations at 100 Mc/s and 9400 Mc/s during run 5. In this case, as shown in figure 19, the 9400 Mc/s phase follows the refractivity quite closely throughout the entire period, while the 100 Mc/s path length variations show large departures associated with sunrises and sunsets. This is taken to indicate that the 9400 Mc/s path is essentially free of ground-reflection (because of the greater effective roughness at the shorter wavelength), while the 100 Mc/s path includes a significant reflected component. Again, a change in the vertical difference in refractivity of the order of a few N-units over a height of about 45 meters would be required to produce the observed effect. In view of the nature of the path, this again is considered a reasonable change to be expected.

Comparisons of the spectra of phase fluctuations at 100 Mc/s and 9400 Mc/s are shown in figures 41 and 42. Since the data at each frequency have been normalized to parts per million, similar spectral distributions would be indicated by coincidence of the two sets of curves. The absence of such coincidence is interpreted to indicate that the major noise in the measuring system is in the phase measuring section. Because of the difference in radio frequencies, a given error in the measurement of path length variance at 100 Mc/s corresponds to an error  $(94)^2$ , or 8800 times as large at 9400 Mc/s. Thus, we should expect the 100 Mc/s spectrum to flatten out at a level about 4 decades higher than that of the 9400 Mc/s spectrum. This is, in fact, observed in figure 42. At the lower frequencies, however, the signal-to-noise ratio improves and the 100 Mc/s and 9400 Mc/s spectra tend to coincide.

These results are interpreted to indicate that the only significant effect of frequency (in the region 100 - 9400 Mc/s) is the result of differences in multipath behavior. In other words, in the absence of multipath, the behavior of two frequencies would be very nearly alike. The introduction of multipath adds a frequency-sensitive mechanism which can produce significant changes in signal behavior.

## 2.7. Path Length Difference Data

Run 8, over a 17.1 km path at Cape Canaveral, involved the use of two antennas at one terminal, separated vertically by 7 meters. The upper antenna (19 m above ground) was located at or very near the radio horizon, while the lower one was probably well below the radio horizon.

The long-term variations in path (phase) difference are plotted in figure 43. They are expressed here as variations in apparent elevation angle in milliradians and in wavelengths of path difference. For purposes of comparison, the surface refractivity is also shown. The range

of the elevation angle variation over the 2-day period is about 1 milliradian. This appears to be fairly well correlated with the surface refractivity. Some further analysis of these long-term data has been made by Bean and Thayer [1963]. Figure 26 shows the power spectrum of the apparent path length variations occurring on the upper path. Figure 44 shows the corresponding spectrum for the lower path variations, which were recorded only during the first half of the experiment. Comparison of these two figures shows a very high correlation in the time variations in the upper and lower path spectra. The corresponding median spectra for both upper and lower paths are plotted in figure 45. The shapes of the spectra are similar on both paths and are the same at night as during the day in spite of the sizeable diurnal variation in the level of both spectra. It would also appear that the absolute level of variance on the upper path is somewhat higher than on the lower path, but because of the analysis repeatability problems mentioned before, it is considered unwise to make closer than orders-of-magnitude comparisons of absolute spectral density levels observed on any two variables.

The time varying spectrum of path difference is plotted in figure 46. Since these variations represent changes in the apparent angular position of the remote site as observed by this 24-foot vertical baseline system, the spectral densities are expressed in terms of milliradians. Figure 47 shows the corresponding median power spectra for day and night. If the variations on the upper and lower paths were uncorrelated over the whole passband, the path difference spectrum would have the same slope and same diurnal variation in level as the single path spectra. However, the path difference spectrum is relatively low at 0.1 c/s, indicating that at the lower frequency end there are components of the single-path variations which are positively correlated, thereby reducing the variance of their difference.

The diurnal variations pattern of the path difference spectrum is reversed, with higher spectral densities during the night. This suggests that the upper and lower path variations were more nearly correlated during the day than at night. This may be caused by the vertical movement of convective currents during the day which would tend to synchronize refractive index variations on the two vertically separated paths. On the other hand, horizontal stratification of the atmosphere at night would tend to reduce the correlation.

### 3. Conclusions

The results of these experiments suggest the following conclusions:

1. The long-term variations in phase (apparent path length) are well-correlated with refractivity computed from standard meteorological data recorded at the path terminals.

2. The spectral density of phase variations in the fluctuation frequency range from 0.1 up to 10 cycles per second may vary as much as an order of magnitude during a 24-hour period, being generally low at night and high during daytime. The extent of this effect appears to depend on the particular path, since the diurnal variations observed in Colorado were much smaller than those observed in Florida. Of the various meteorological parameters observed, best correlation appears between the spectral density and the wind speed averaged from both terminals.

3. The spectra of phase variations from 0.1 to 10 cycles per second have slopes (on a log-log graph) of approximately -2.2; i. e.,

$$W_{\theta}(f) = kf^{-2.2}.$$

This is somewhat higher than the value of -2.9 observed in the October 1958 measurements. This slope does not appear to vary significantly from day to night or from Florida to Colorado.

4. In the same region of fluctuation frequencies, the intensity of refractivity variations may vary as much as two orders of magnitude between day and night. Again, the daytime values are higher, and this effect is much more pronounced in Florida than in Colorado.

5. The form of the refractivity spectra also shows little effect of time or location, being generally of the form

$$W_N(f) = k' f^{-1.8}$$

Again the exponent is somewhat larger than the average of the October 1958 analyses, e.g. -2.2, but as noted above, this difference probably can be accounted for within the accuracy of the spectral density estimates.

6. Any dependence of the phase variation data on radio signal frequency is believed to be the result of the existence of multipath, which introduces a frequency-dependent mechanism.

## 4. Appendix

### 4.1. Tower Motion Study

The experiments at Cape Canaveral all involved mounting one or more of the antennas used in the apparent path length measurements on a tower made of aluminum scaffolding. Since the system is capable of recording very small changes in apparent path length (on the order of 0.003 mm), it was necessary to determine the extent to which the data were effected by motion of the tower itself. To do this, during the September 1959 run the apparent path length variations occurring over a short (30 meter) path were recorded simultaneously with those occurring over the long path. The physical arrangement is shown in figure 8. The short path extended from the same antenna on the tower used in the long path measurements to another antenna mounted about one meter above ground and 30 meters from the base of the tower. The path was made as short as possible in order to minimize the apparent changes in length caused by the atmosphere as opposed to actual changes caused by tower movement.

Figure 48 shows the time variations in the apparent path length spectrum observed on this short path. Comparing this with the long path spectrum in figure 25, we find the diurnal pattern is very similar in both cases, indicating that most of the variations observed on the short path in this range of spectral frequencies were probably caused by refractive index variations rather than by tower movement. Figure 49 shows the median spectra of the short path and long path variations, both plotted in terms of parts per million of the long path. It is evident that the short path length spectrum is at least an order of magnitude smaller than the long path spectrum in the frequency range 0.1 to 1 c/s. Between 1 and 10 c/s this margin of safety drops to as low as 3 to 1. However, since most of the short path length variations in this frequency

range appear to be atmospheric in origin, it is very unlikely that the long path variation data were significantly contaminated by tower movement.

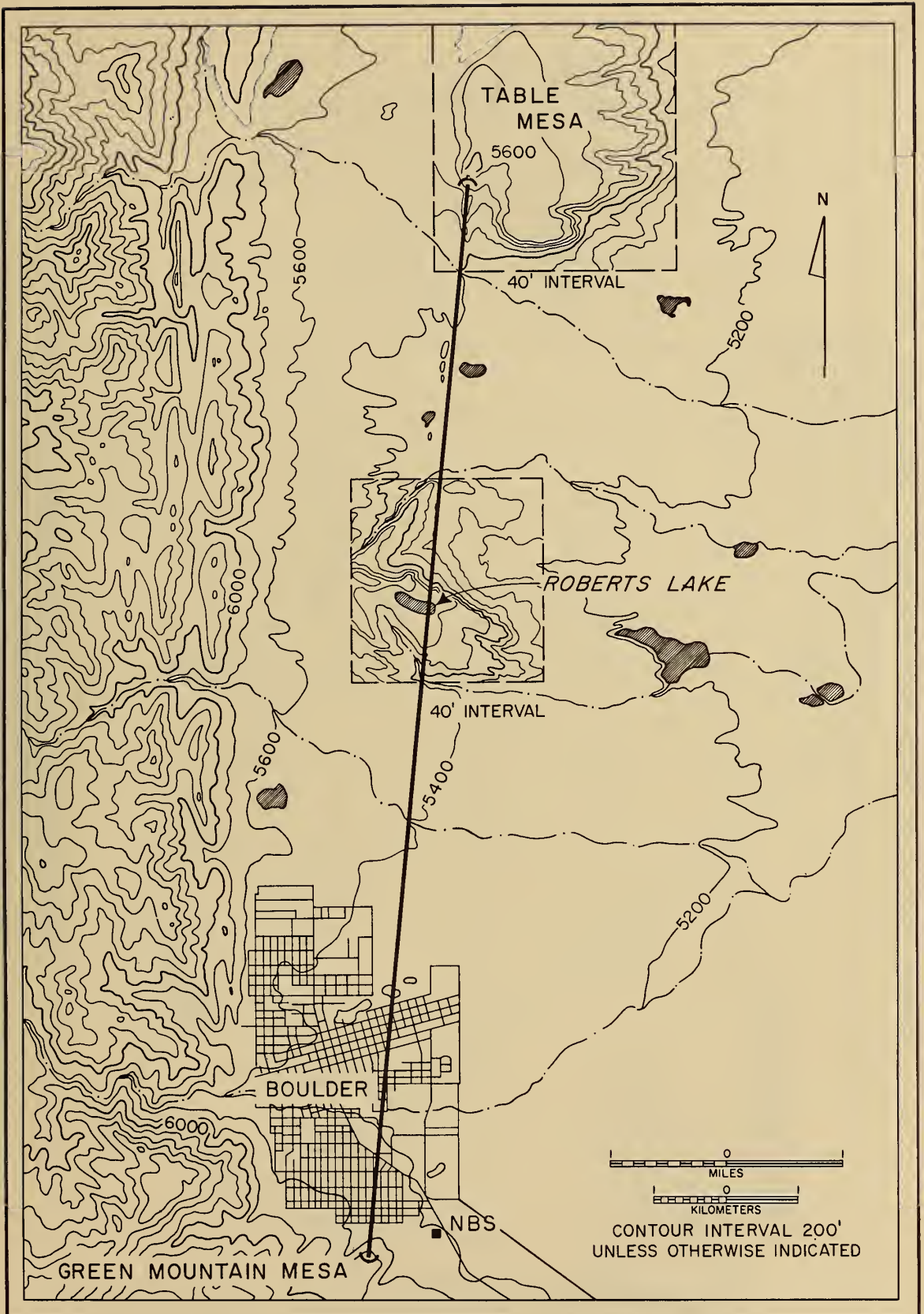
The long-term (hour-to-hour) variations in the short path length, on the other hand, appear to be more closely correlated with actual tower movements than with refractive index changes. Figure 50 shows these variations compared to the corresponding long-term changes in air temperature and refractivity. The coefficient of correlation between the short path length and refractivity is 0.16, while the correlation of path length with air temperature is 0.66. This suggests that most of the long-term path length changes on the short path can be ascribed to differential thermal expansion of the tower and guy cables.

It should be noted that the maximum change in the short path length was only about 1 mm, or a little over 1 part in  $10^7$  of the long (7.7 km) path. Thus, the tower movements could not have contributed a readable error to the long-term, long path variations shown in figure 20.

## 5. References

- Bean, B. R., and G. D. Thayer (May - June 1963). Comparison of observed atmospheric radio refraction effects with values predicted through the use of surface weather observations, Radio Sci. J. Res. NBS/USNC-URSI 67D, No. 3, 273-285.
- Blackman, R. B., and J. W. Tukey (1958). The measurement of power spectra from the point of view of communication engineering, Bell System Tech. J., Parts 1, 2, 37, 185 and 485.
- Thompson, M. C., Jr., H. B. Janes, and A. W. Kirkpatrick (January 1960). An analysis of time variations in tropospheric refractive index and apparent radio path length, J. Geophys. Res. 65, No. 1.
- Thompson, M. C., Jr., and H. B. Janes (July-August 1959). Measurements of phase stability over a low-level tropospheric path, Radio Sci. J. Res. NBS/USNC-URSI 63D (Radio Prop.), No. 1
- Thompson, M. C., Jr., and M. J. Vetter (February 1958). Single-path phase measuring system for three-centimeter radio waves, Rev. Sci. Instru. 29, No. 2, 148-150.





GREEN MOUNTAIN MESA - TABLE MESA PATH

Figure 1

TERRAIN PROFILE OF GREEN MOUNTAIN MESA - TABLE MESA PATH

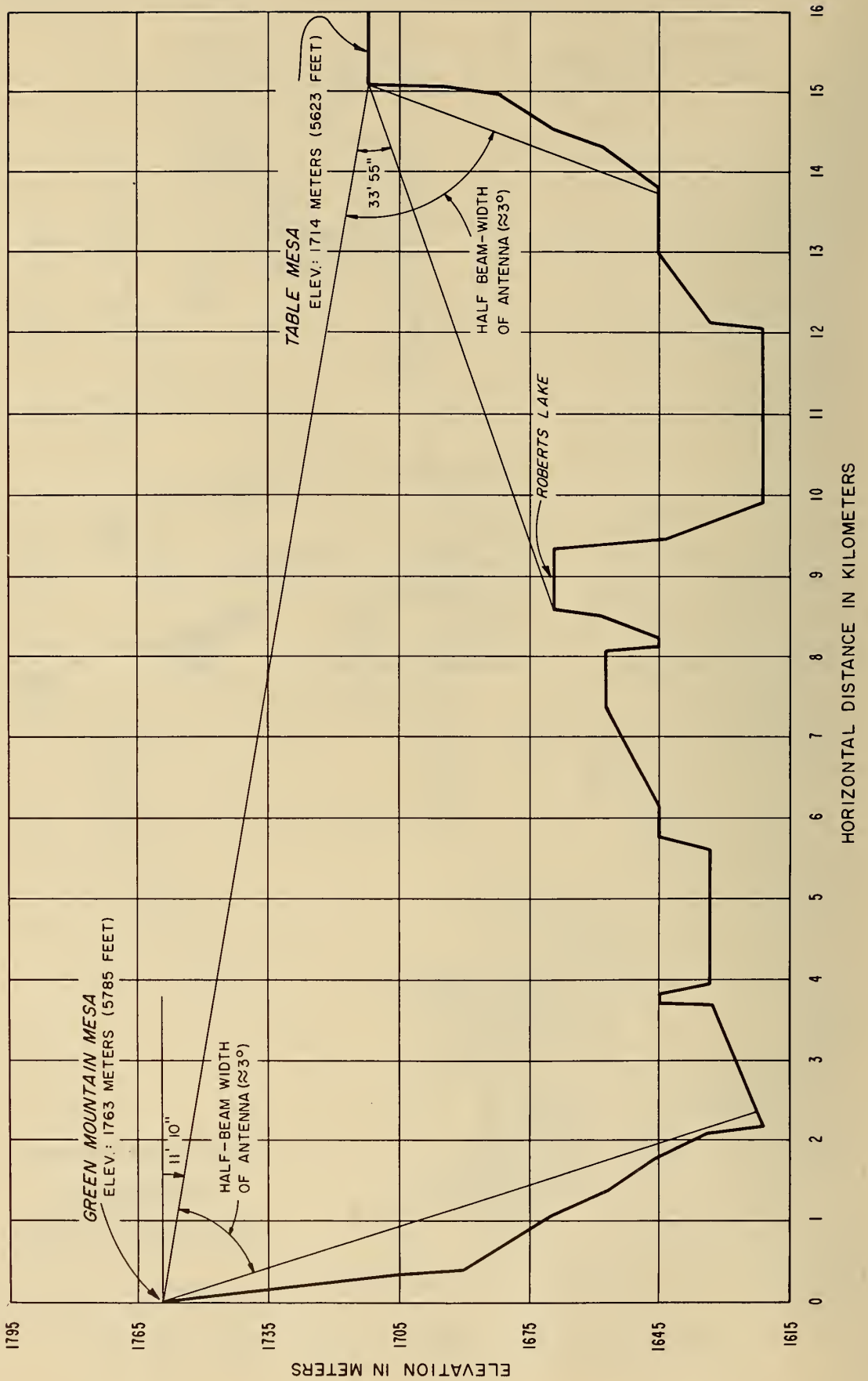


Figure 2

CONTOUR MAP TABLE MESA SITE  
713 m PATH

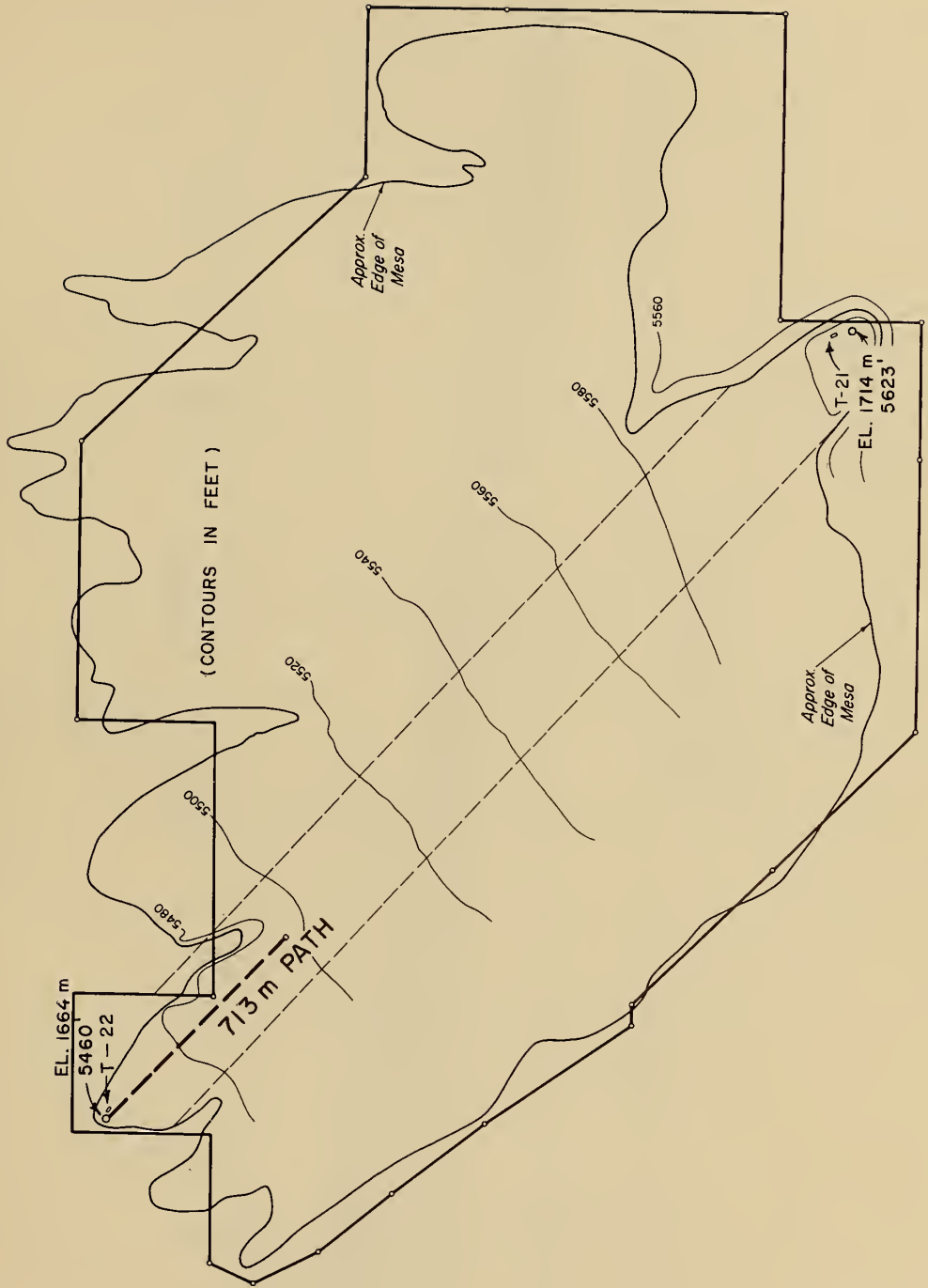


Figure 3

PROFILE, 713 m PATH  
TABLE, MESA SITE

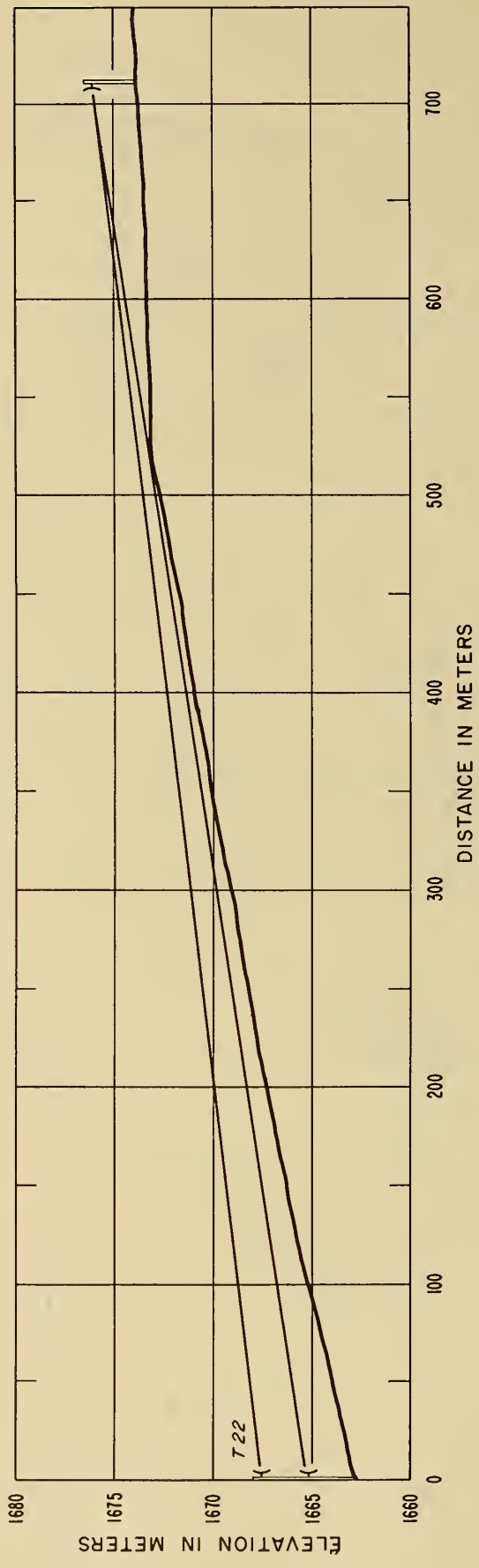


Figure 4

CONTOUR MAP TABLE MESA SITE  
3.2 km PATH

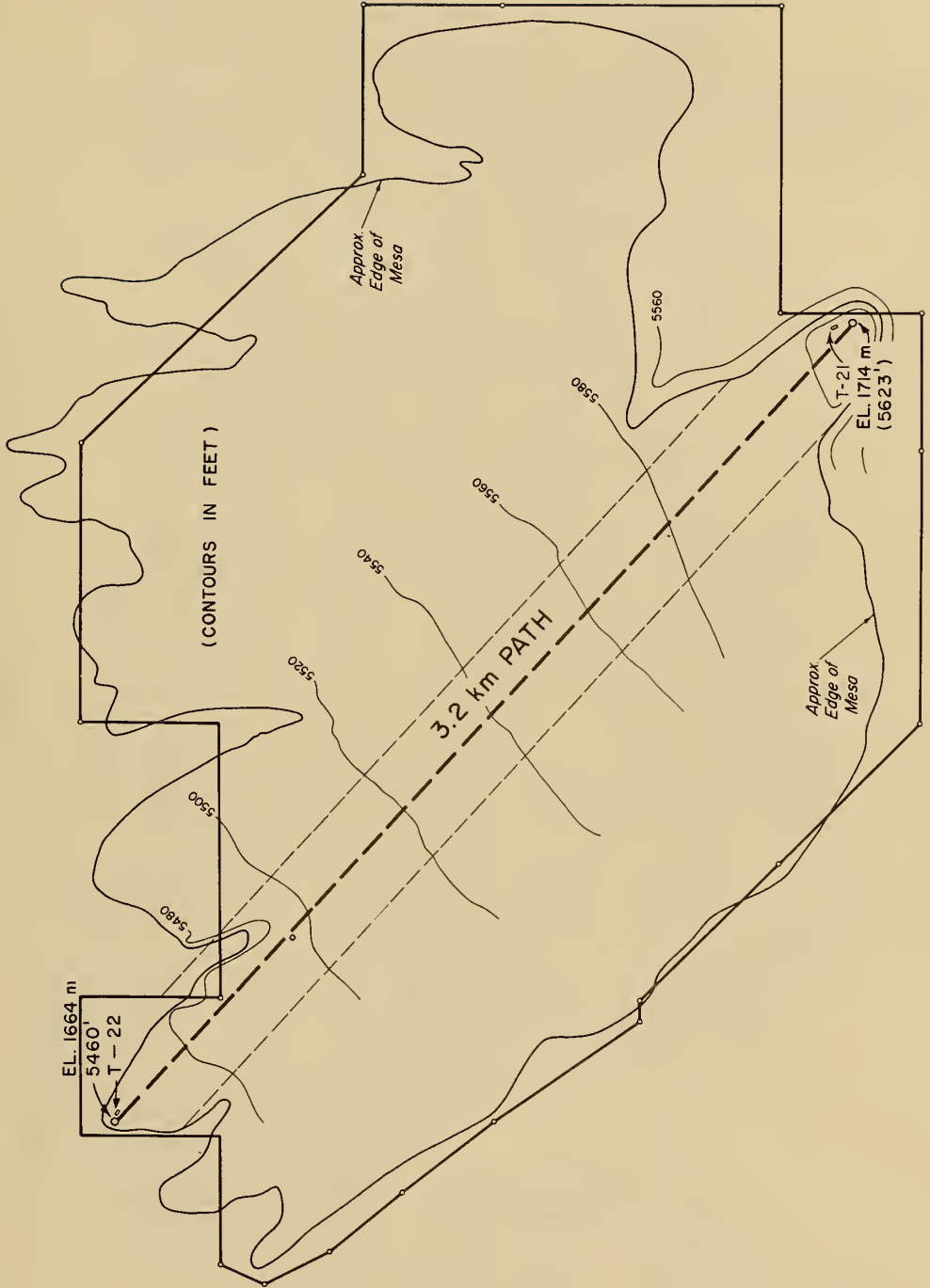


Figure 5

PROFILE , 3.2 km PATH  
TABLE MESA SITE

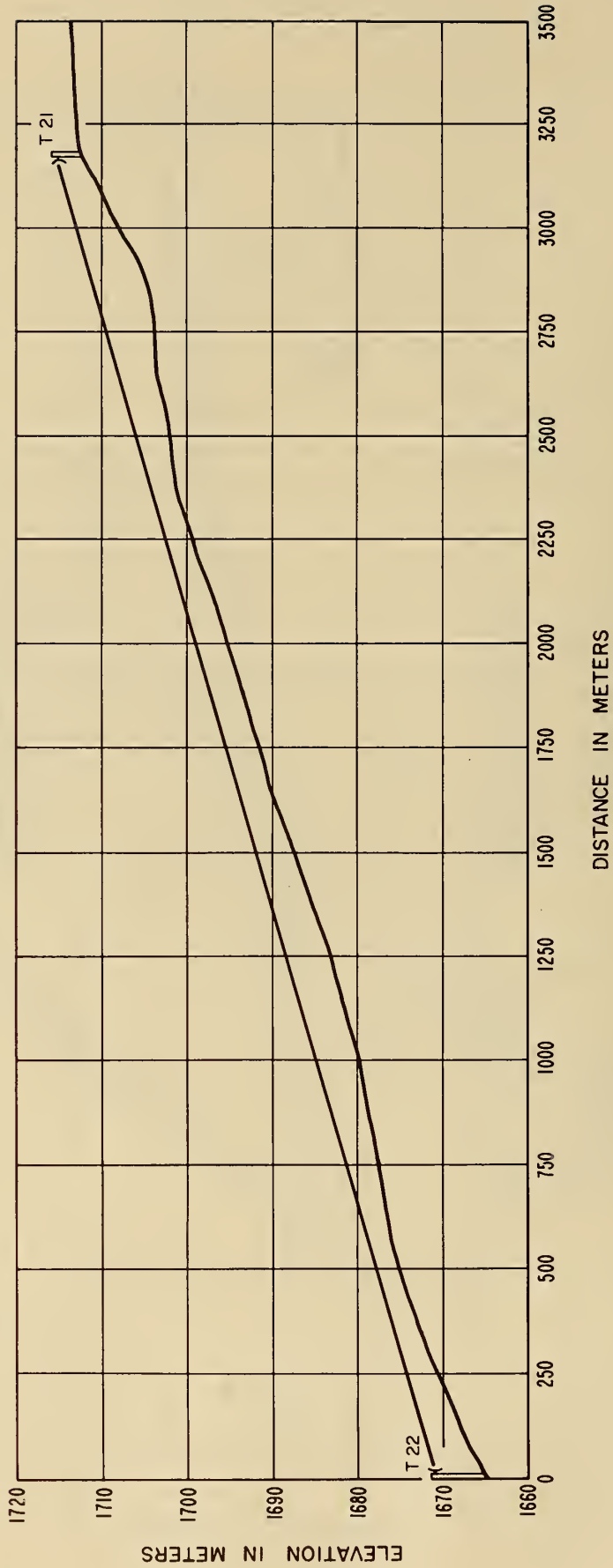


Figure 6

CONTOUR MAP - CAPE CANAVERAL, FLORIDA  
7.7 km PATH

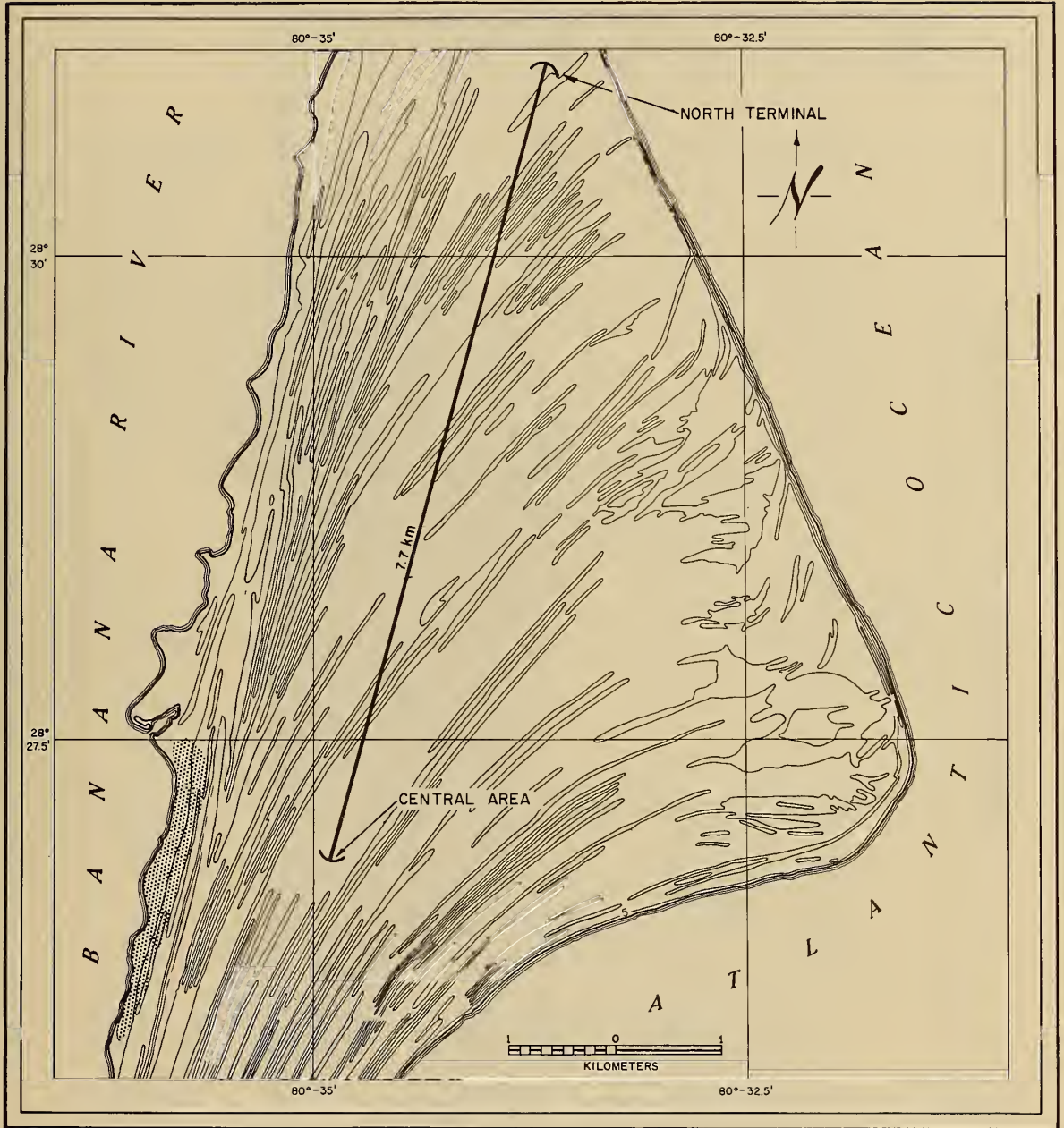


Figure 7

PROFILE OF 8 km PATH: CAPE CANAVERAL

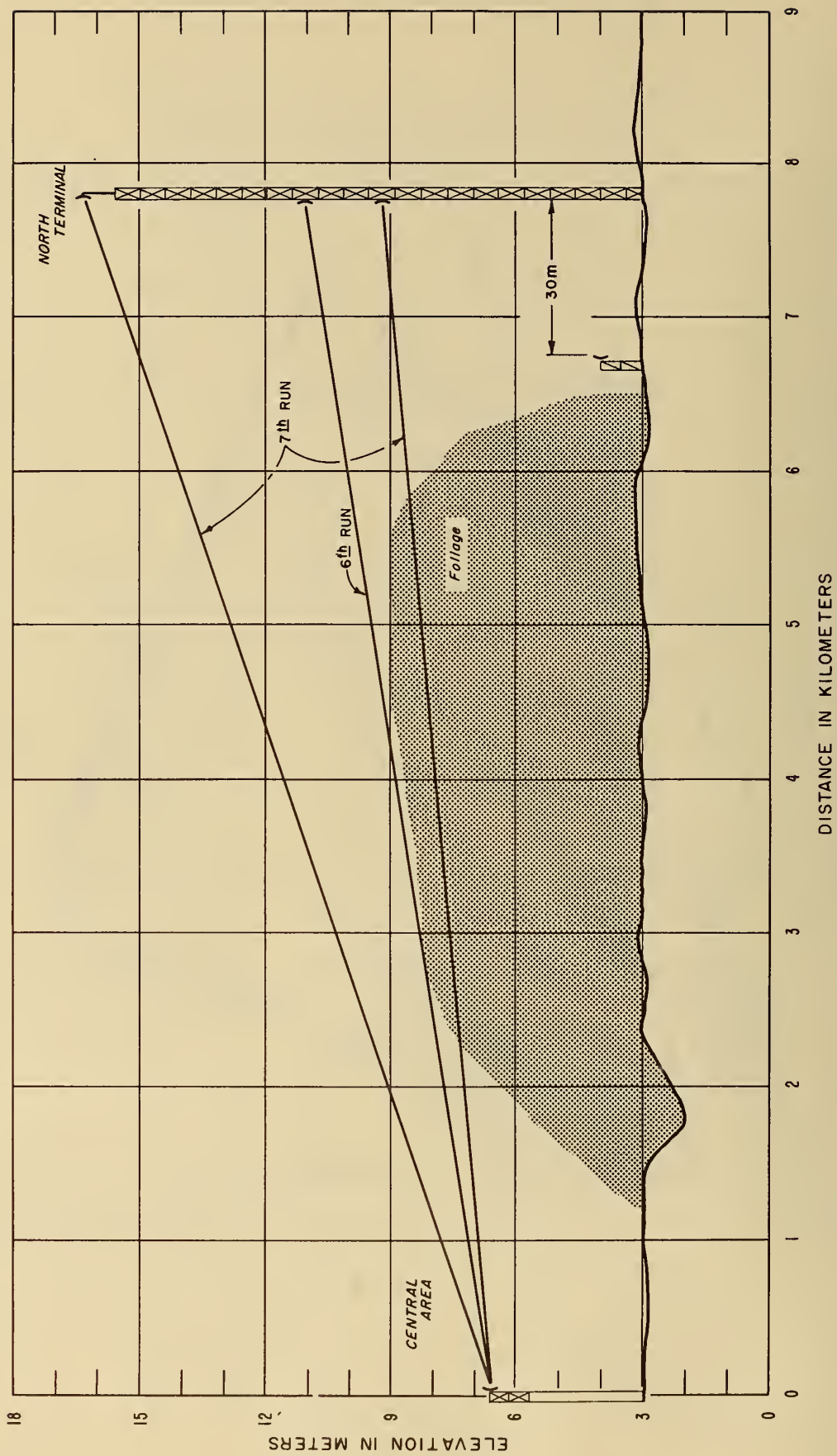
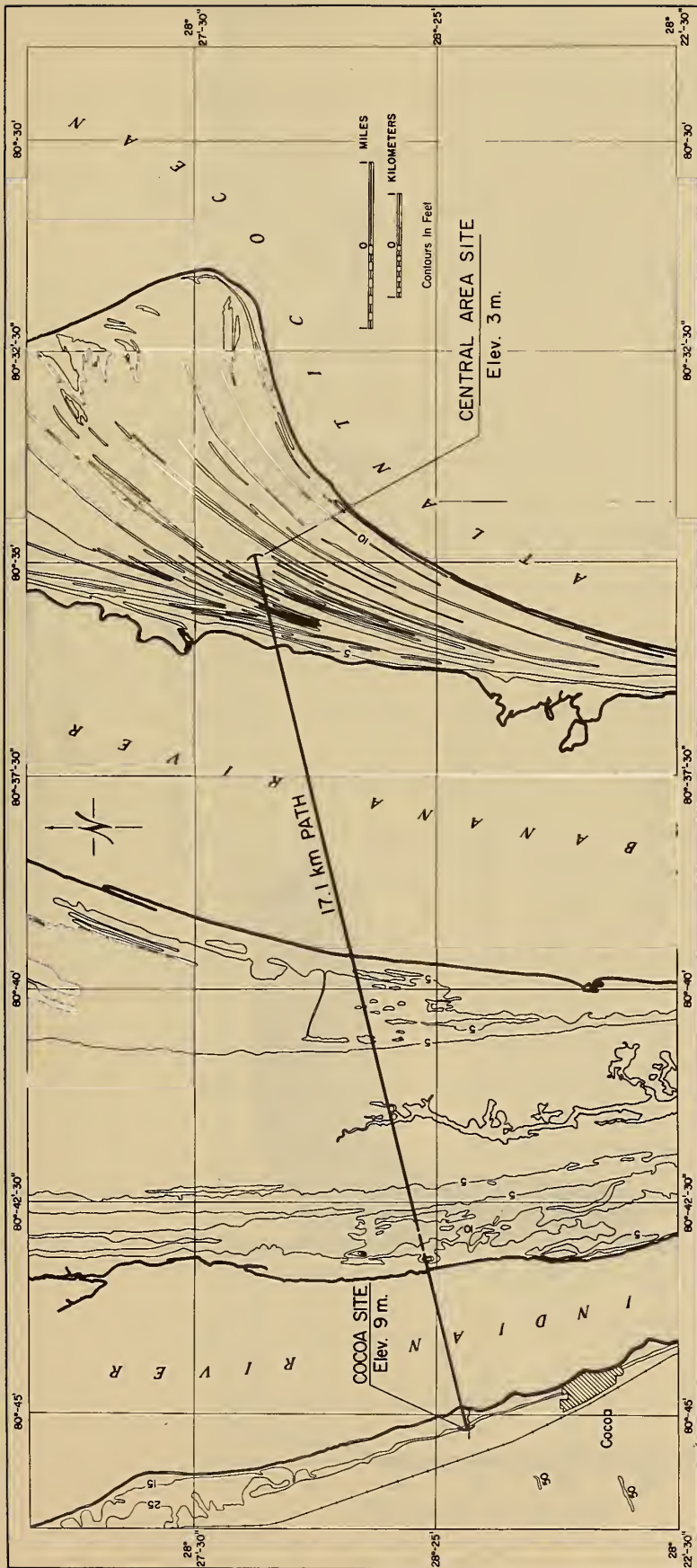


Figure 8



CONTOUR MAP - CAPE CANAVERAL - COCOA, FLORIDA

Figure 9

PROFILE OF 17.1 km PATH: CAPE CANAVERAL - COCOA, FLORIDA

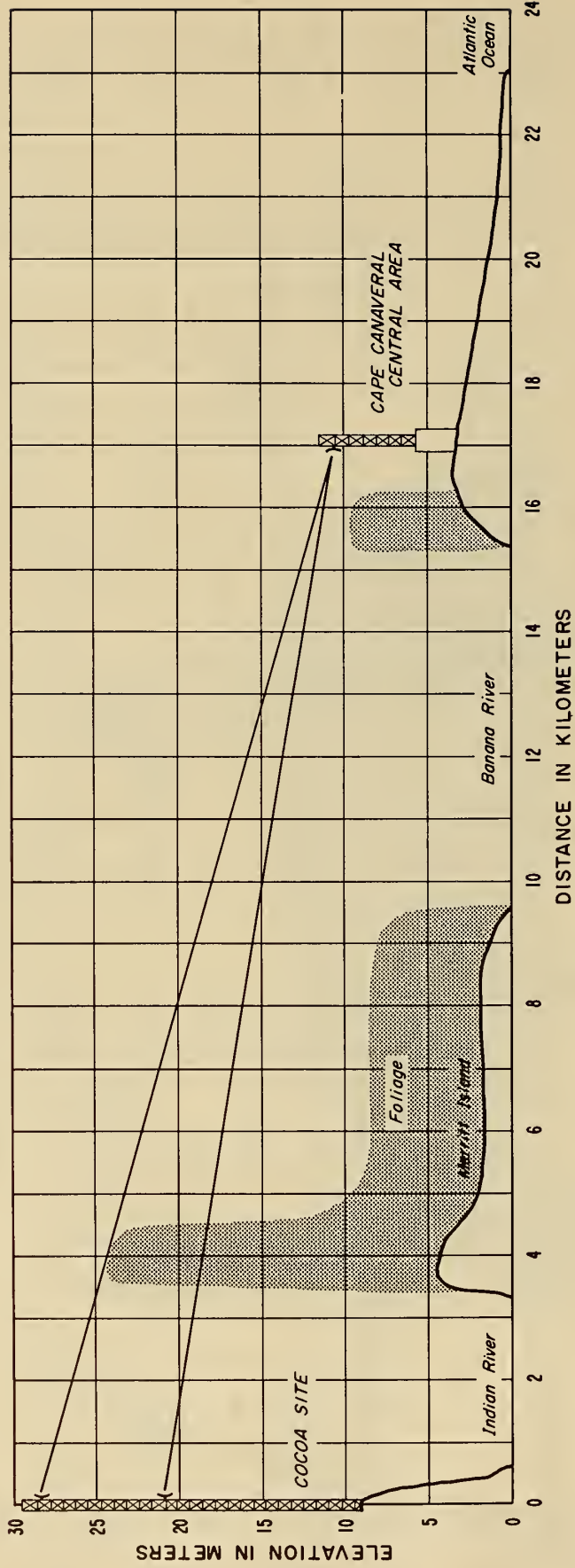


Figure 10

EXAMPLES OF APPARENT PATH LENGTH VARIATIONS OBSERVED  
AT CAPE CANAVERAL, FLORIDA

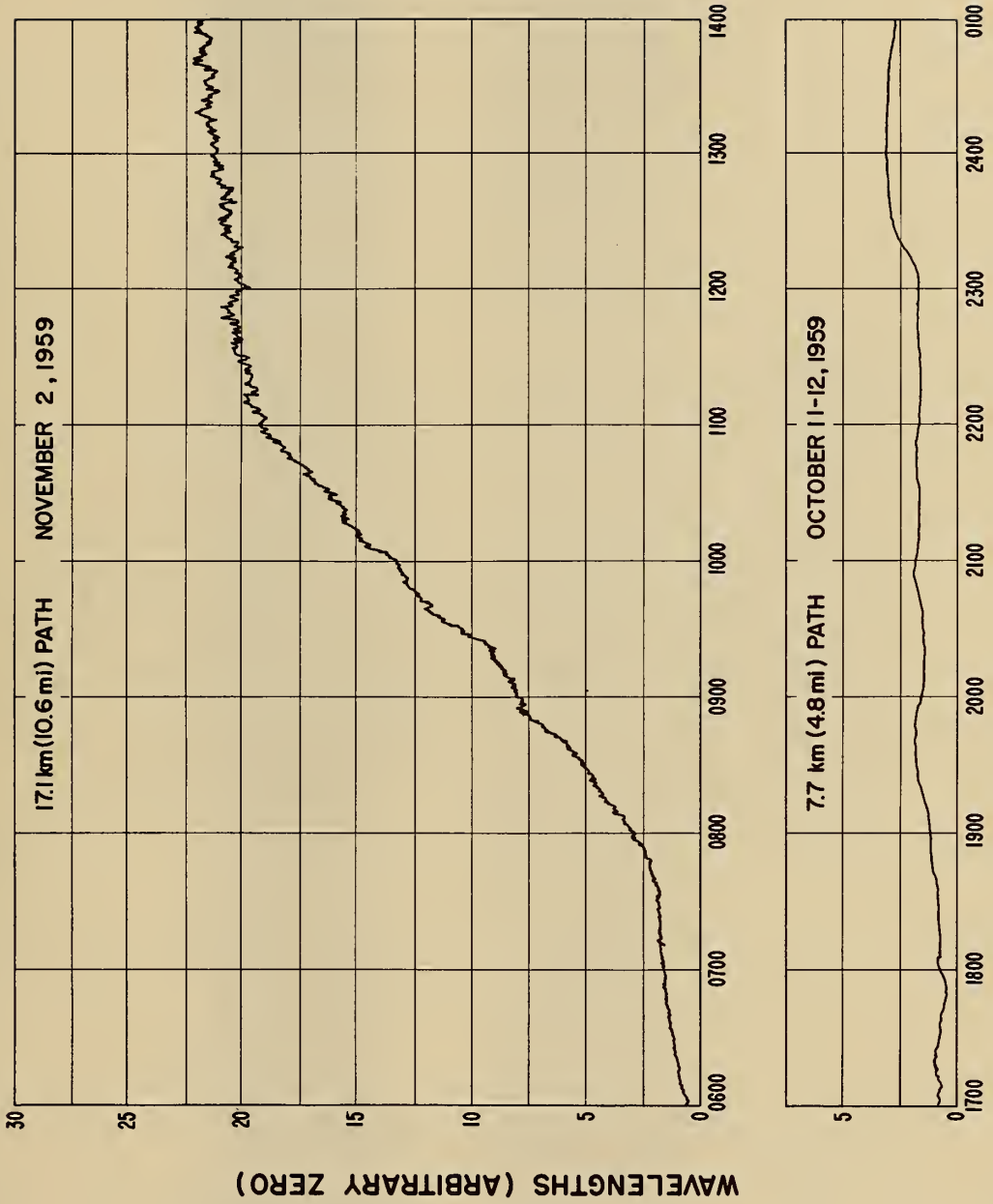
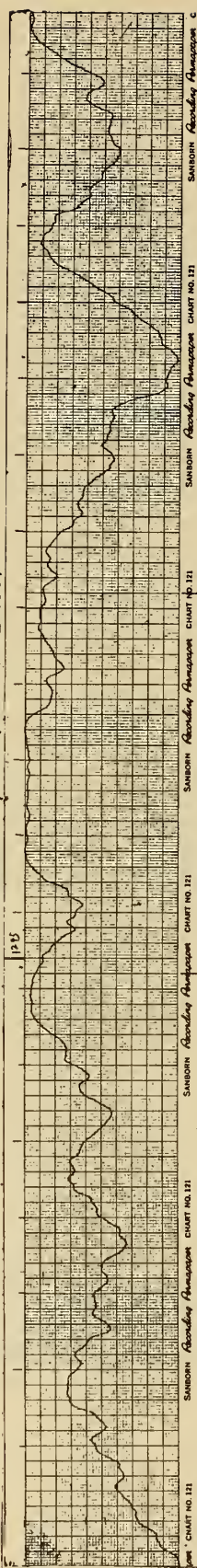


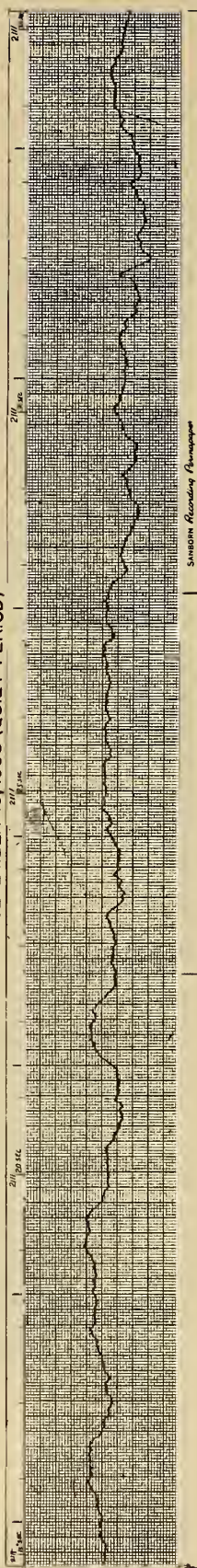
Figure 11

EXAMPLES OF BAND-PASS RECORDING  
 OF APPARENT PATH LENGTH VARIATIONS  
 15.2 km (9.4 mi) PATH BOULDER, COLORADO  
 9400 MC

1245 SEPTEMBER 15, 1958 (ACTIVE PERIOD)



2111 SEPTEMBER 16, 1958 (QUIET PERIOD)



NOTE DIFFERENT  
 SCALES

Figure 12

EXAMPLES OF APPARENT PATH LENGTH VARIATIONS OBSERVED  
ON 15.2 km (9.4 mi) PATH AT BOULDER, COLORADO  
JULY 24, 1959

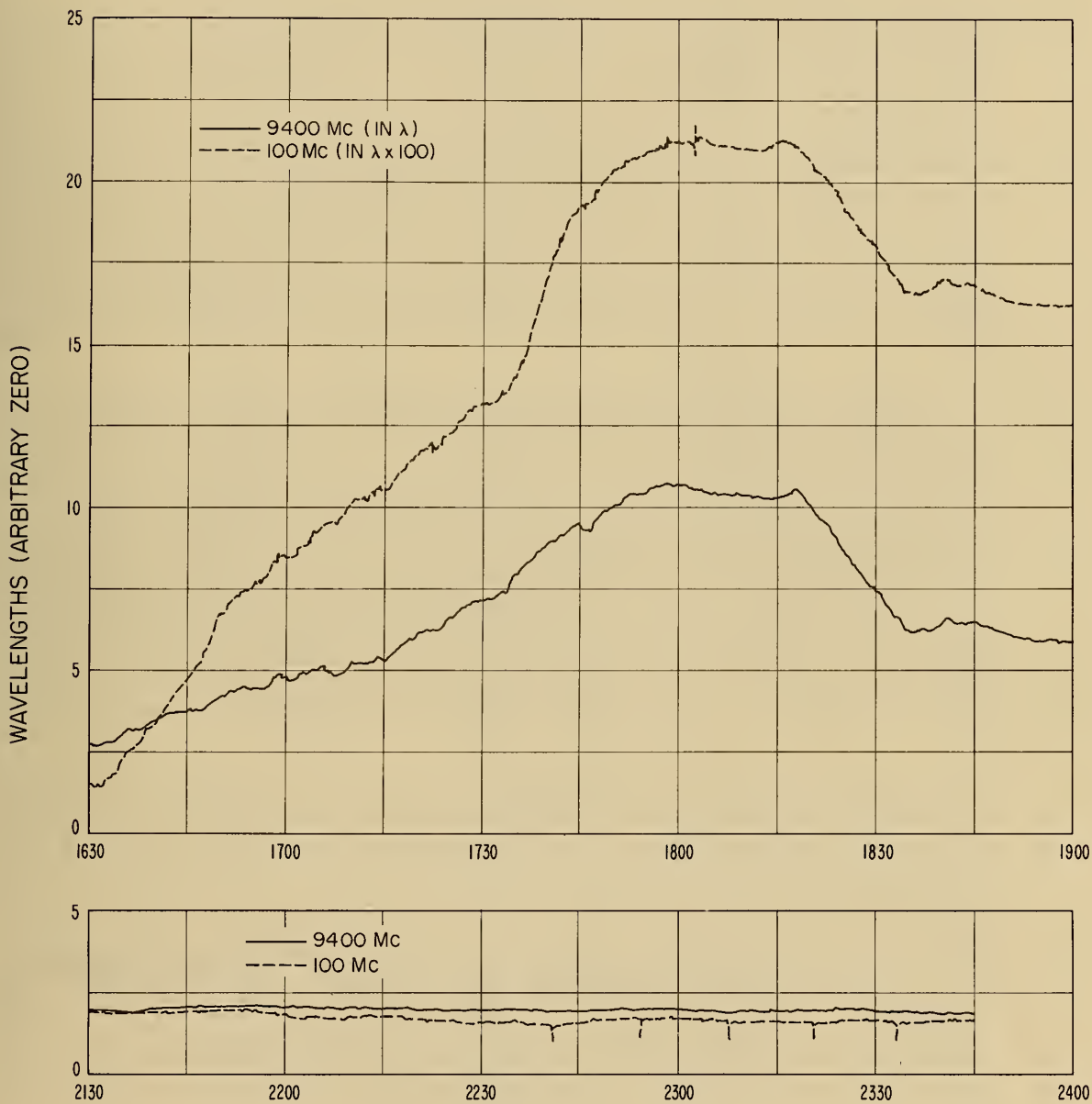


Figure 13

EXAMPLES OF REFRACTIVITY VARIATIONS  
CAPE CANAVERAL, FLORIDA

SEPTEMBER 4, 1959

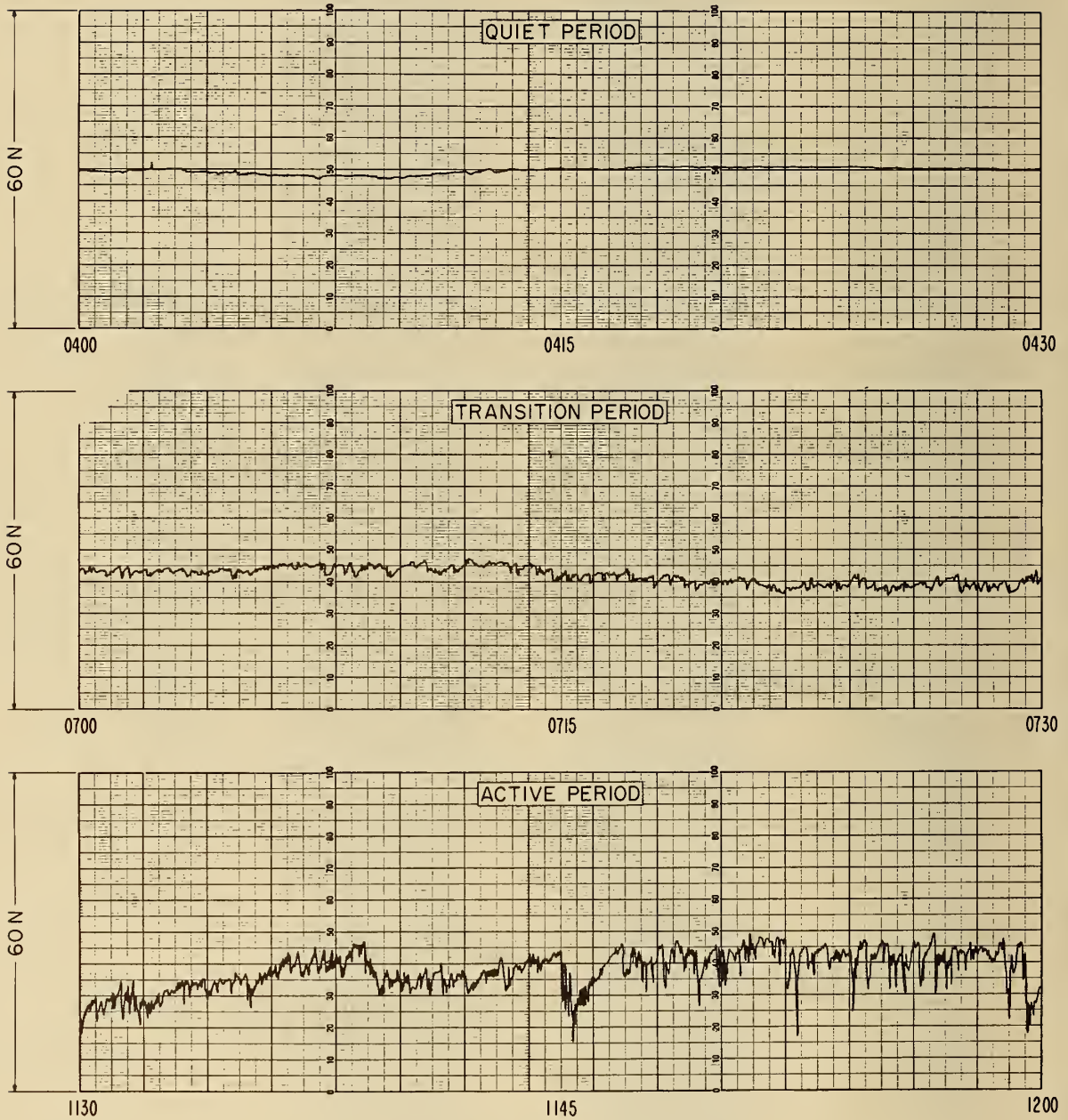


Figure 14

# LONG-TERM VARIATIONS IN APPARENT PATH LENGTH AND RELATED VARIABLES

15.2 km (9.4 mi.) PATH—BOULDER, COLO.—SEPT. 1958

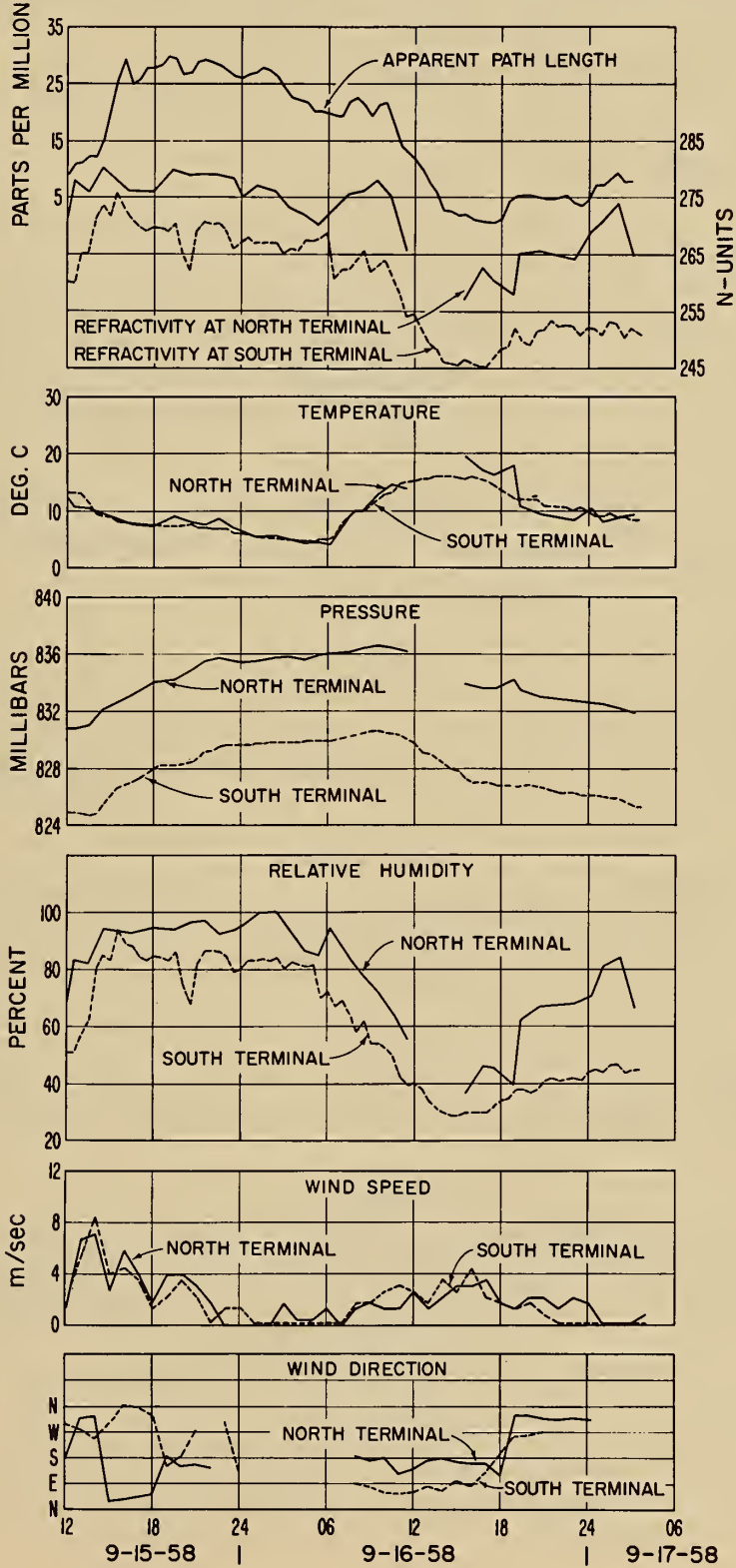


Figure 15

# LONG-TERM VARIATIONS IN APPARENT PATH LENGTH AND RELATED VARIABLES

15.2 km (9.4 mi.) PATH - BOULDER, COLORADO - OCT. 1958

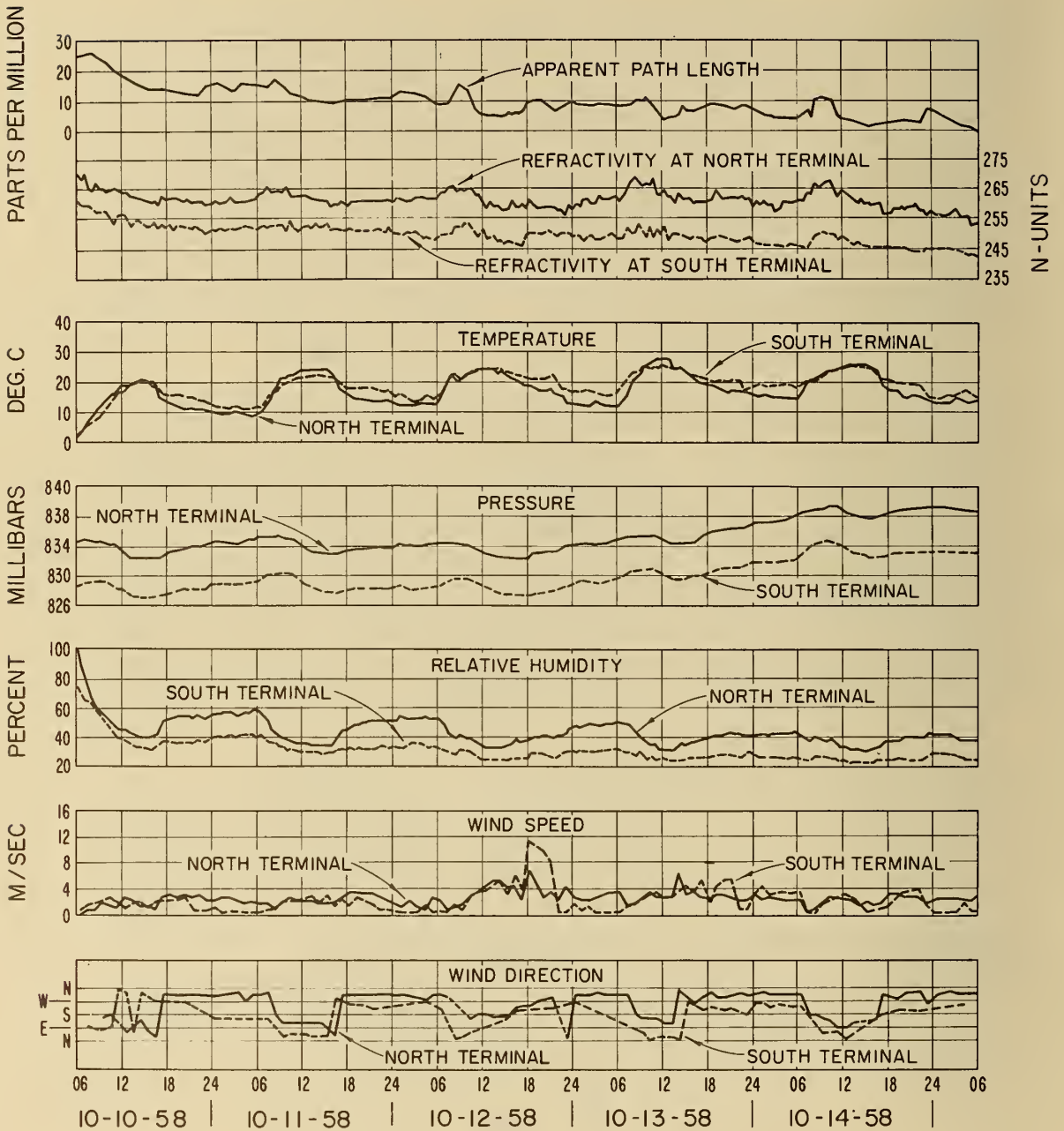


Figure 16

# LONG-TERM VARIATIONS IN APPARENT PATH LENGTH AND RELATED VARIABLES

0.7 km (2340 ft.) PATH - BOULDER, COLORADO, FEBRUARY 1959

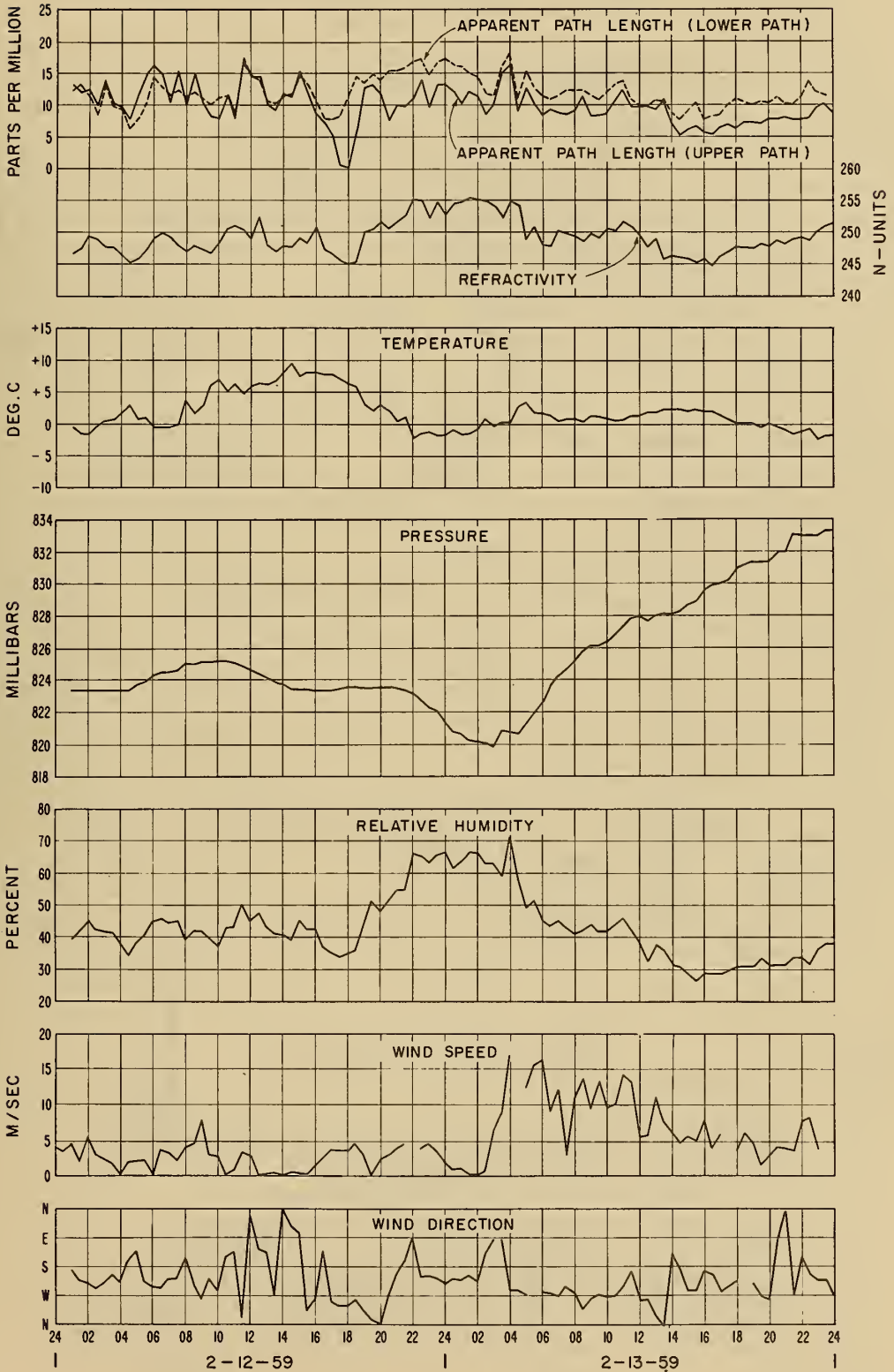


Figure 17

# LONG-TERM VARIATIONS IN APPARENT PATH LENGTH AND RELATED VARIABLES

3.2 km (2 mi.) PATH - BOULDER, COLORADO - JUNE 1959

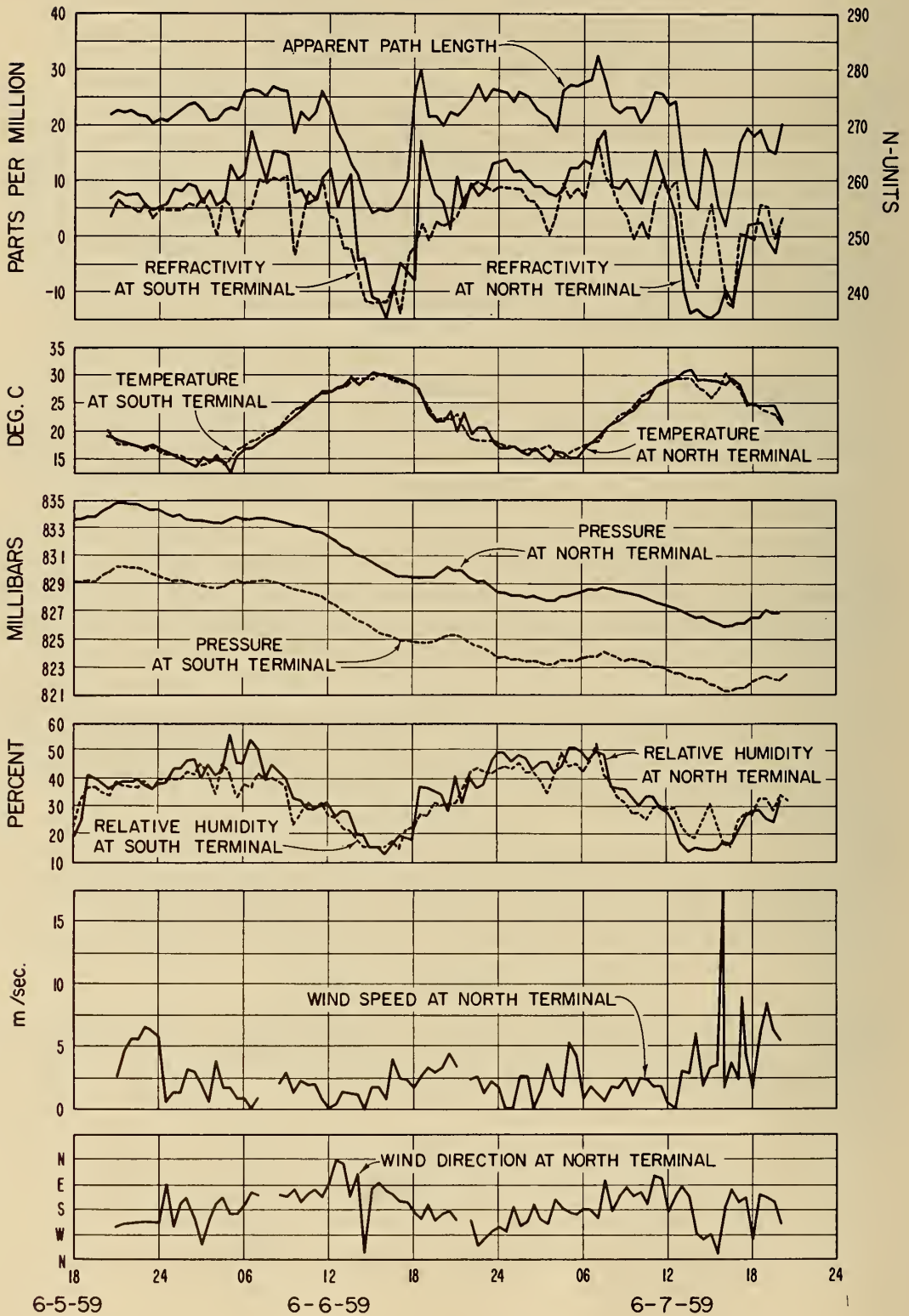


Figure 18

# LONG-TERM VARIATIONS IN APPARENT PATH LENGTH AND RELATED VARIABLES

15.2 km (9.4 mi) PATH, BOULDER, COLORADO JULY 1959

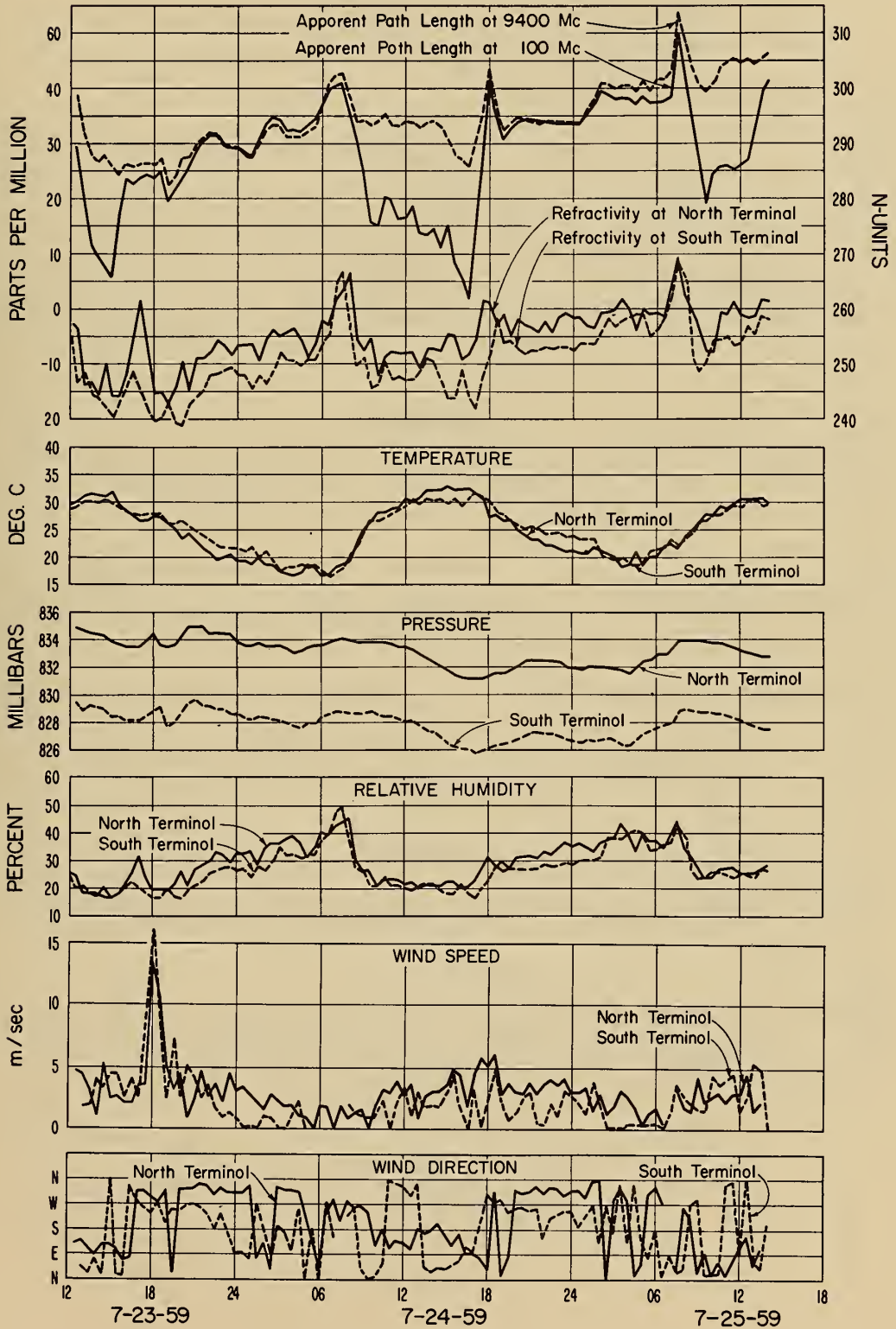


Figure 19

# LONG-TERM VARIATIONS IN APPARENT PATH LENGTH AND RELATED VARIABLES

7.7 km (4.8 mi.) PATH - CAPE CANAVERAL, FLORIDA - SEPT. 1959

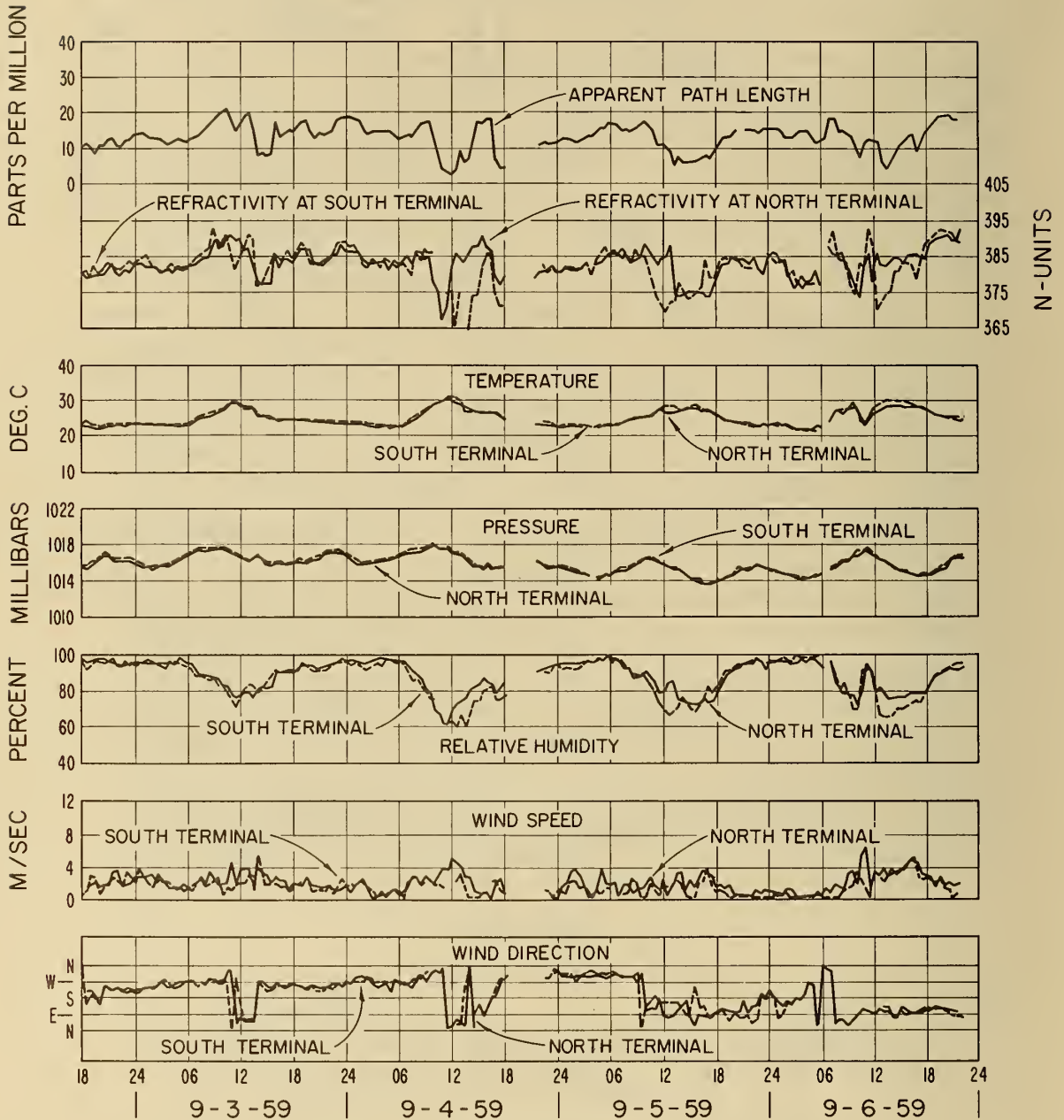


Figure 20

# LONG-TERM VARIATIONS IN APPARENT PATH LENGTH AND RELATED VARIABLES

7.7 km (4.8 mi.) PATH- CAPE CANAVERAL, FLA. - OCT. 1959

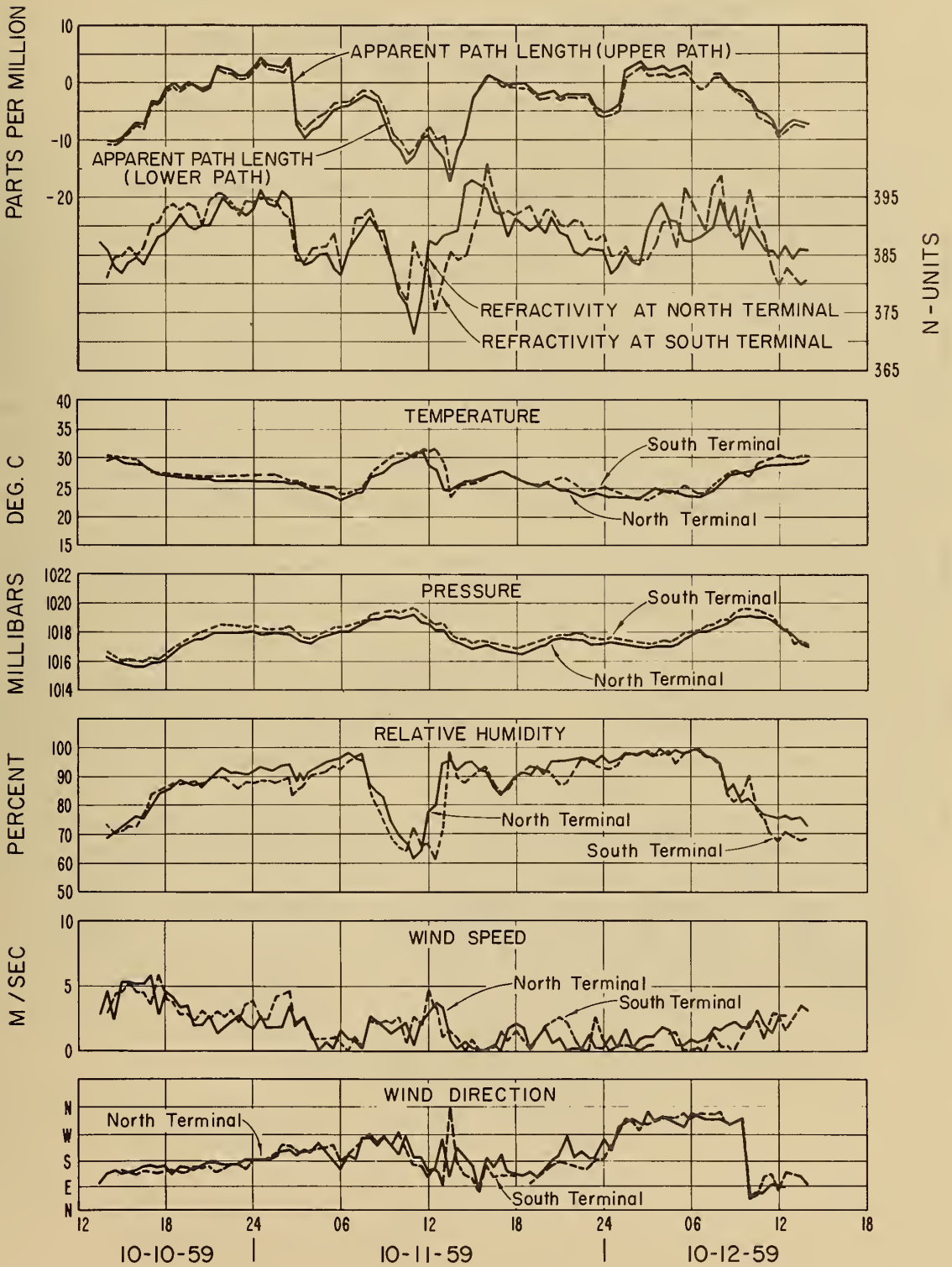


Figure 21

# LONG-TERM VARIATIONS IN APPARENT PATH LENGTH AND RELATED VARIABLES

17.1 km (10.6 mi.) PATH    OCT-NOV, 1959    CAPE CANAVERAL, FLORIDA

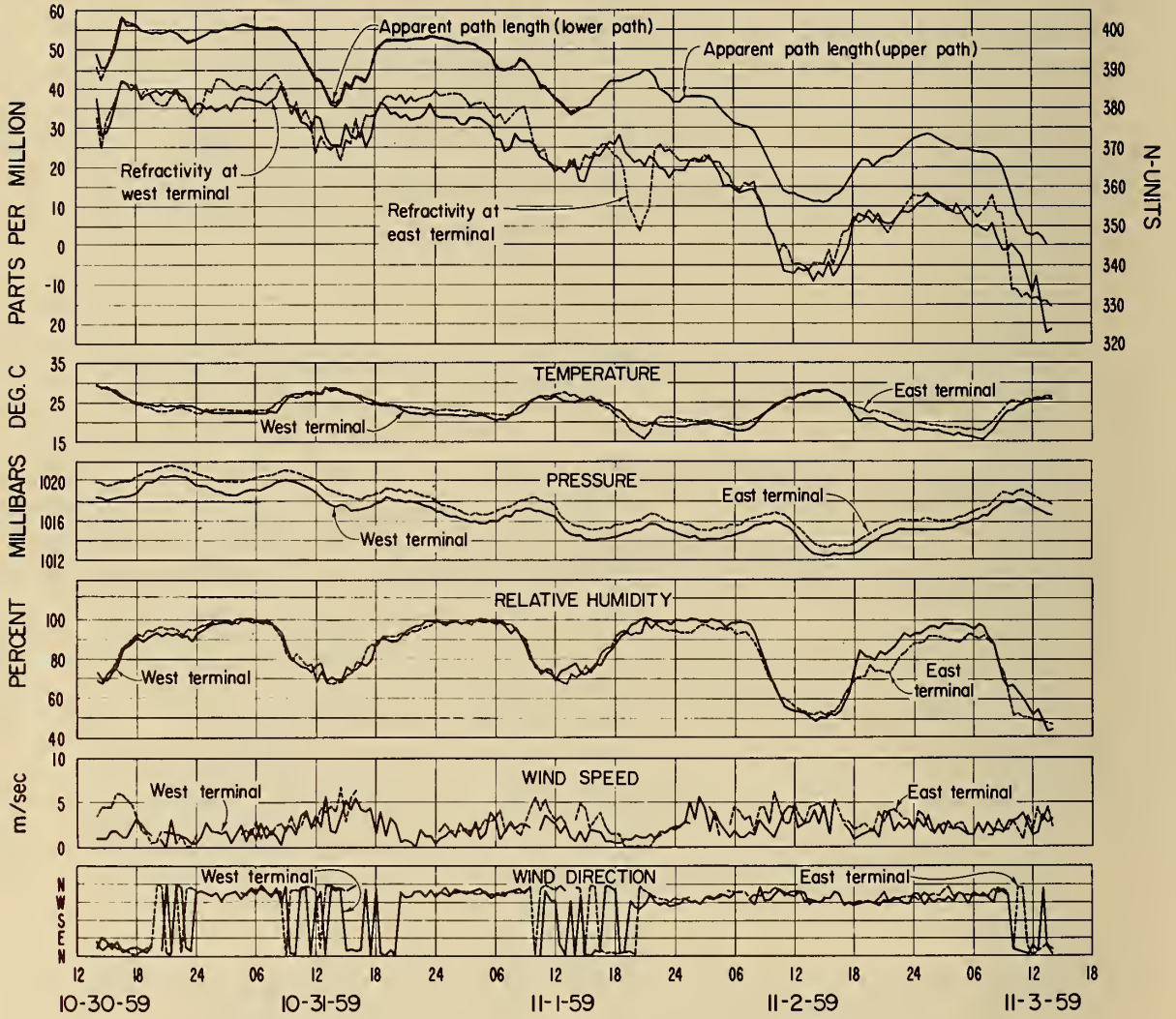


Figure 22

TIME VARIATIONS IN THE POWER SPECTRA  
OF APPARENT PATH LENGTH AND REFRACTIVITY  
3.2 km (2 MI.) PATH AT BOULDER, COLORADO

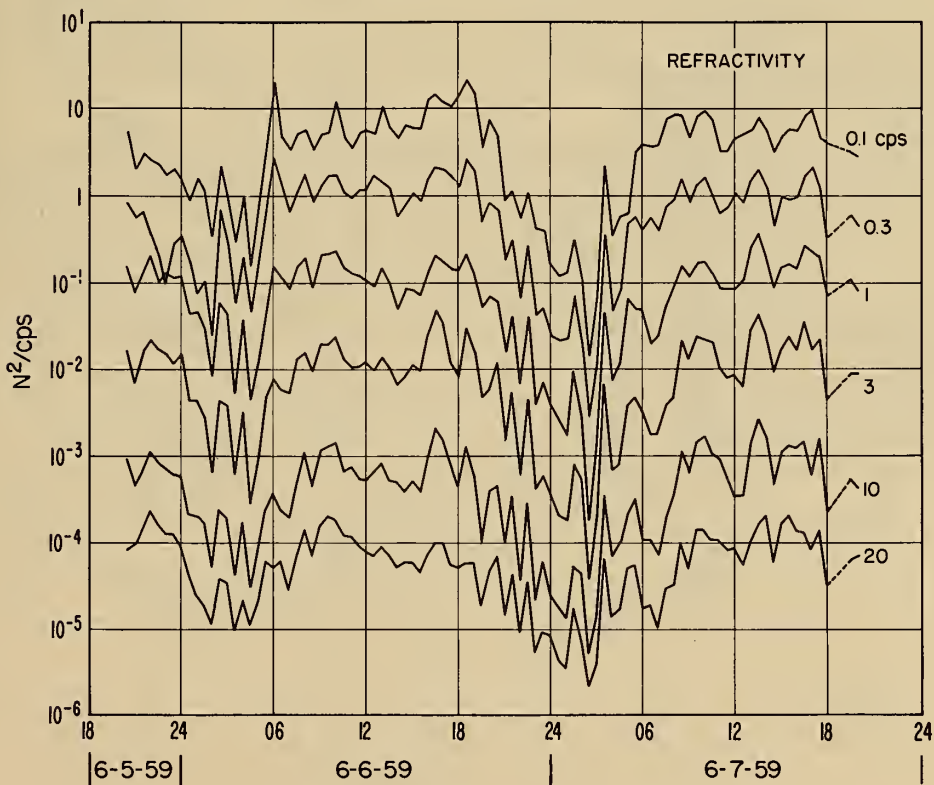
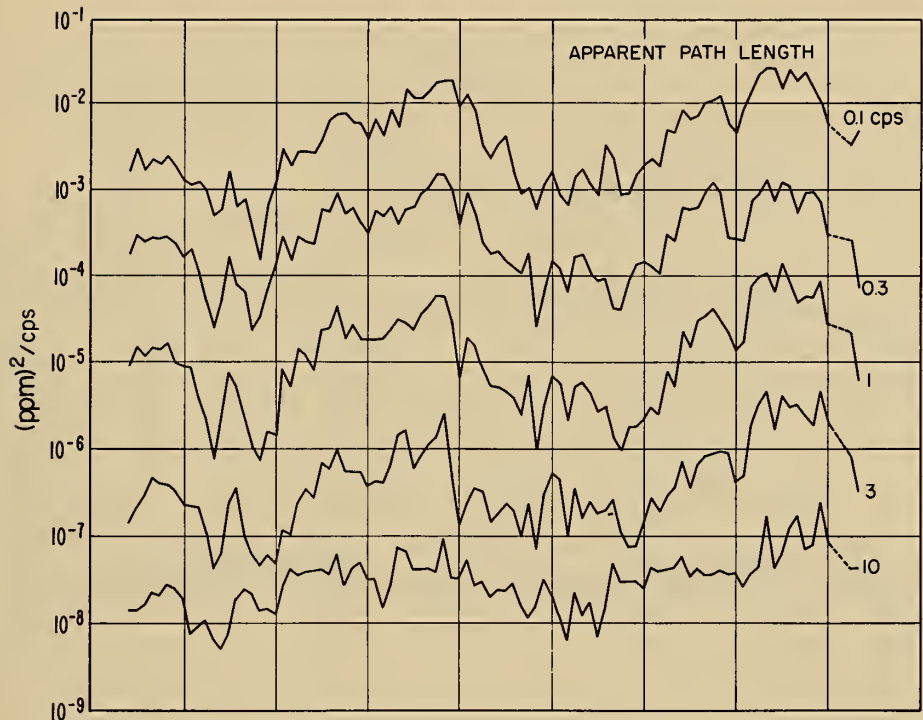


Figure 23

TIME VARIATIONS IN THE POWER SPECTRA OF  
 APPARENT PATH LENGTH AND REFRACTIVITY  
 15.2 km (9.4 mi) PATH, BOULDER, COLORADO

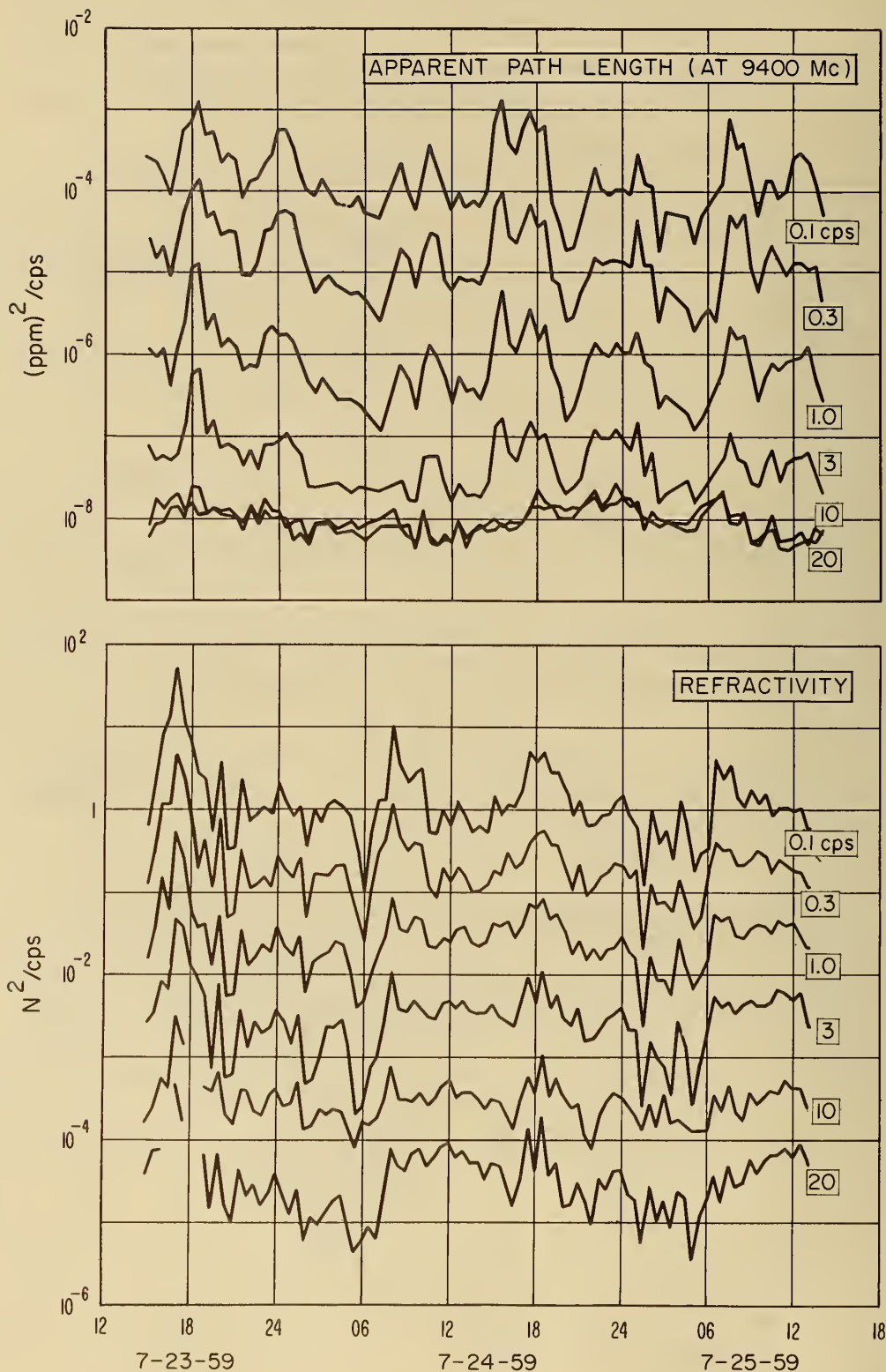


Figure 24

TIME VARIATIONS IN THE POWER SPECTRA  
 OF APPARENT PATH LENGTH AND REFRACTIVITY  
 7.7 km (4.8 mi.) PATH, CAPE CANAVERAL, FLORIDA

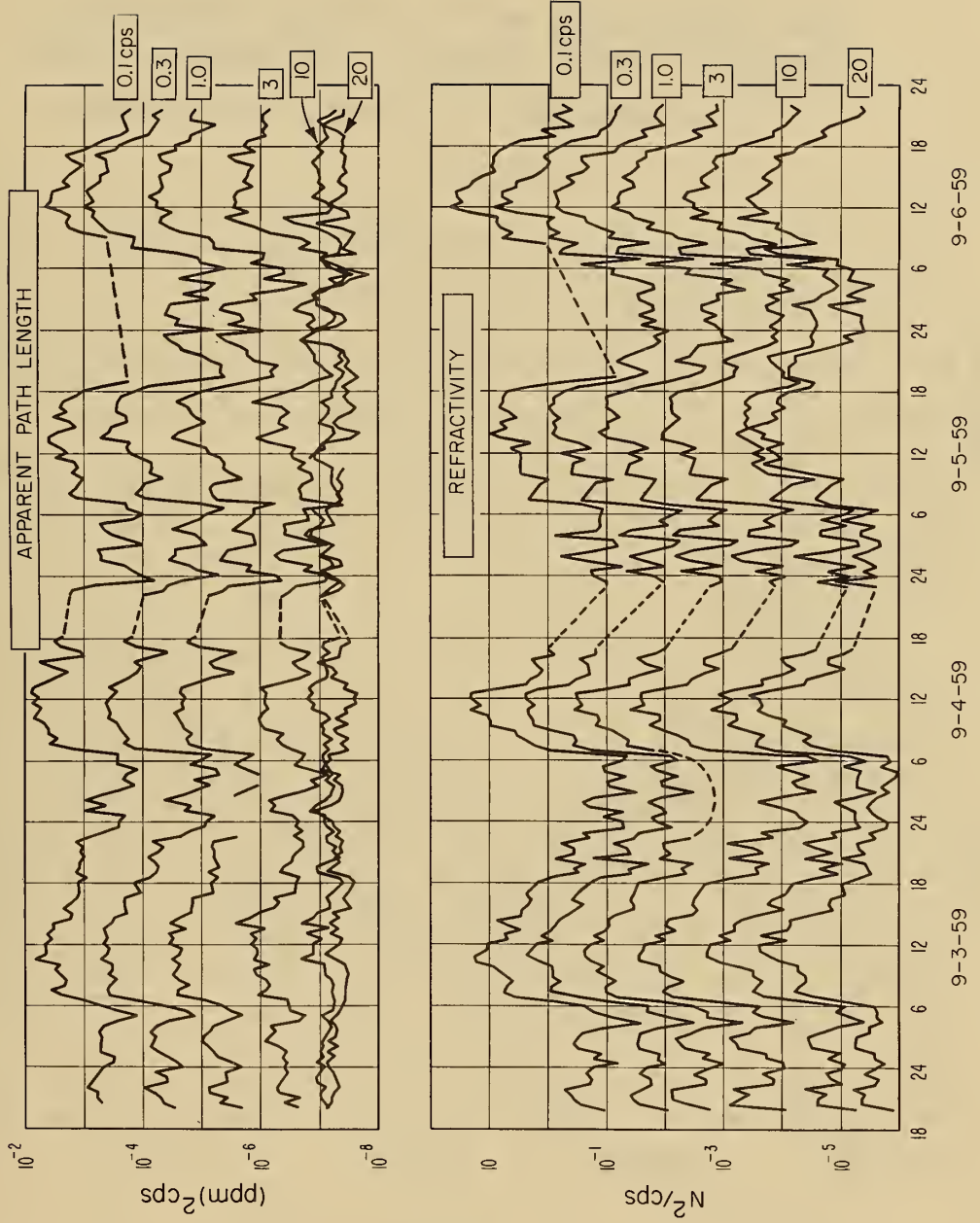


Figure 25

# TIME VARIATIONS IN THE POWER SPECTRA OF APPARENT PATH LENGTH AND REFRACTIVITY

17.1 km (10.6 mi.) PATH AT CAPE CANAVERAL, FLORIDA

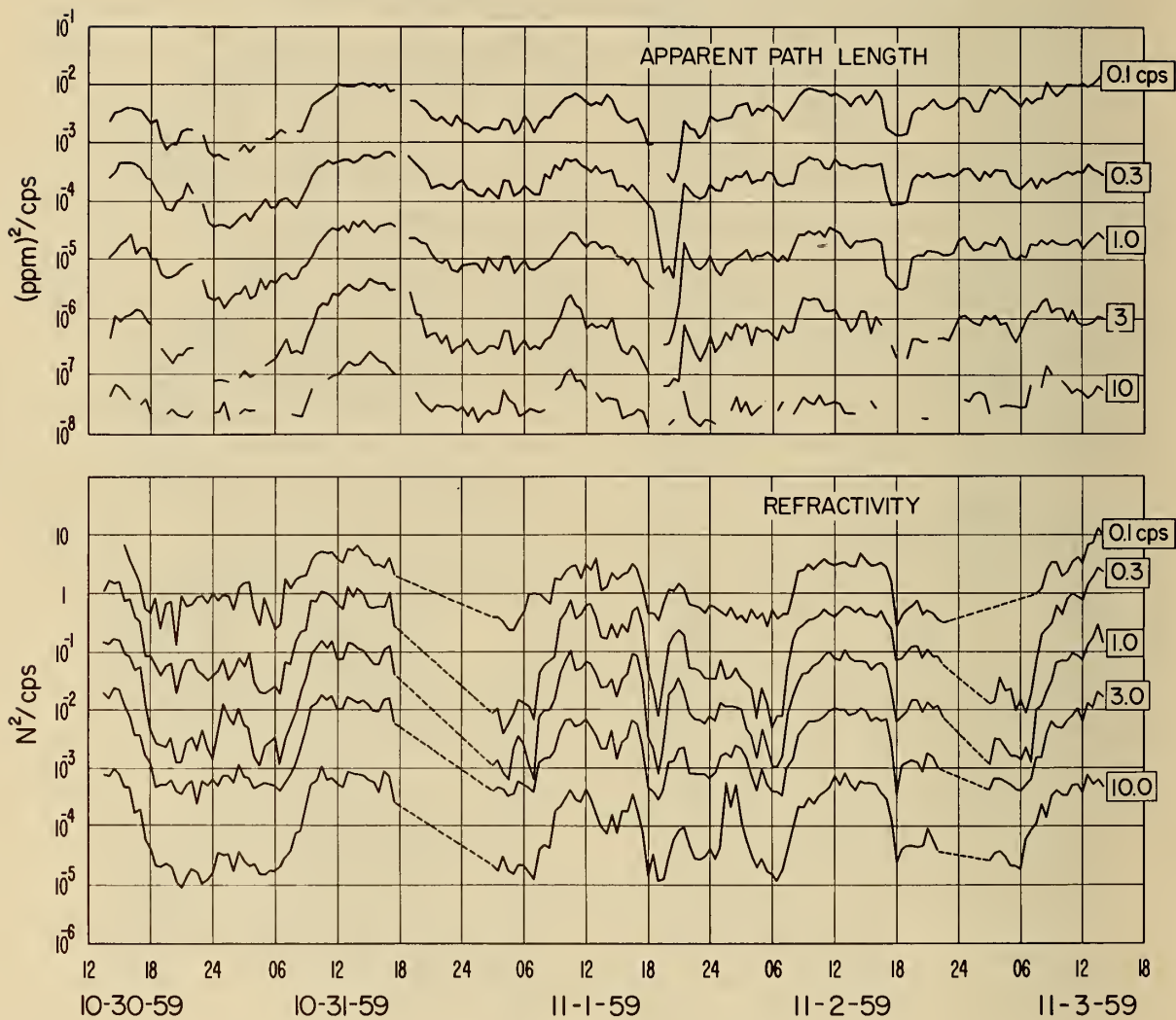


Figure 26

COMPARISON OF SPECTRA OBSERVED IN  
COLORADO AND FLORIDA

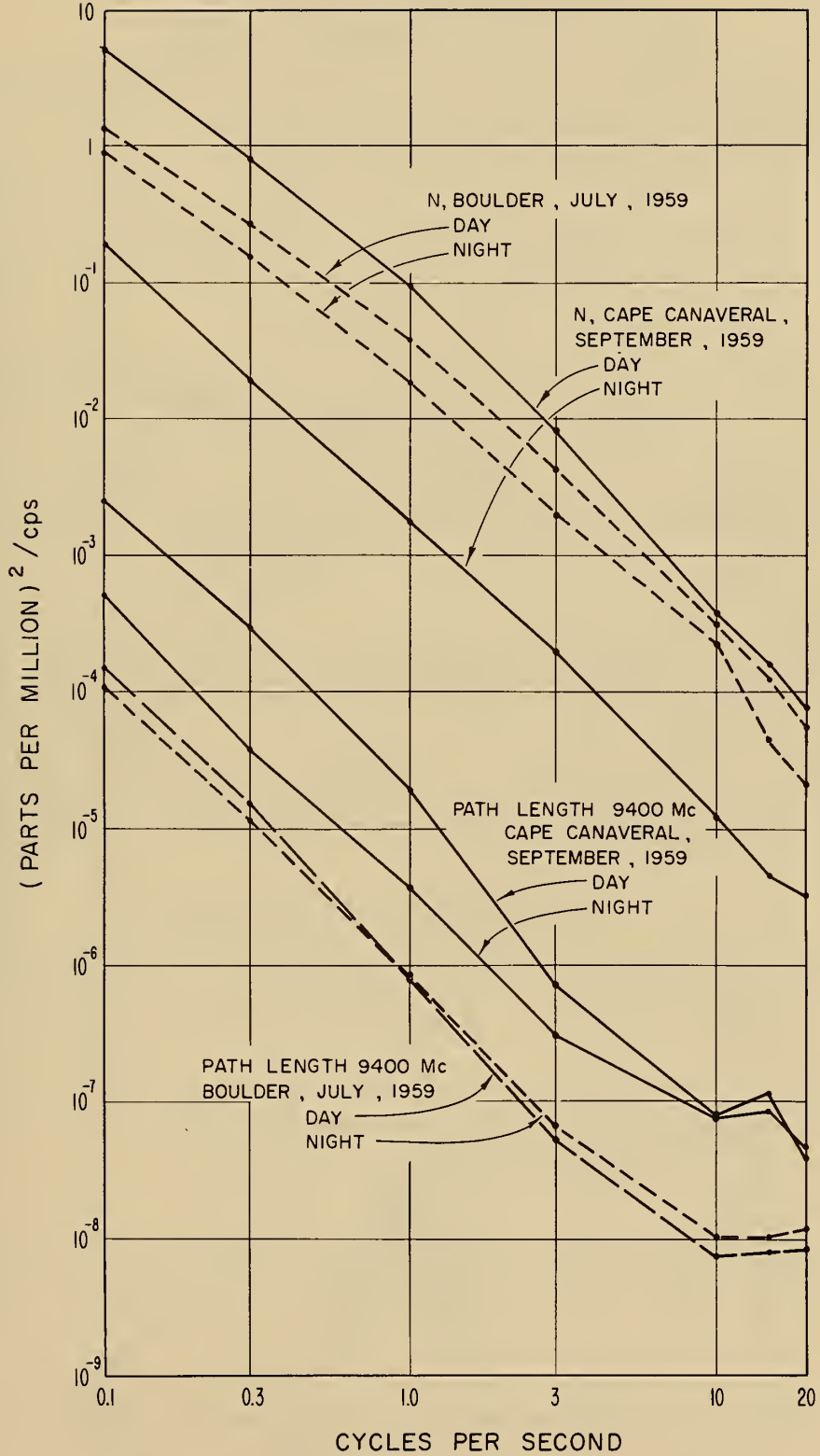


Figure 27

MEDIAN POWER SPECTRA OF APPARENT PATH LENGTH  
AND REFRACTIVE INDEX

3.2 km. (2 MI.) PATH AT BOULDER, COLORADO

JUNE 1959

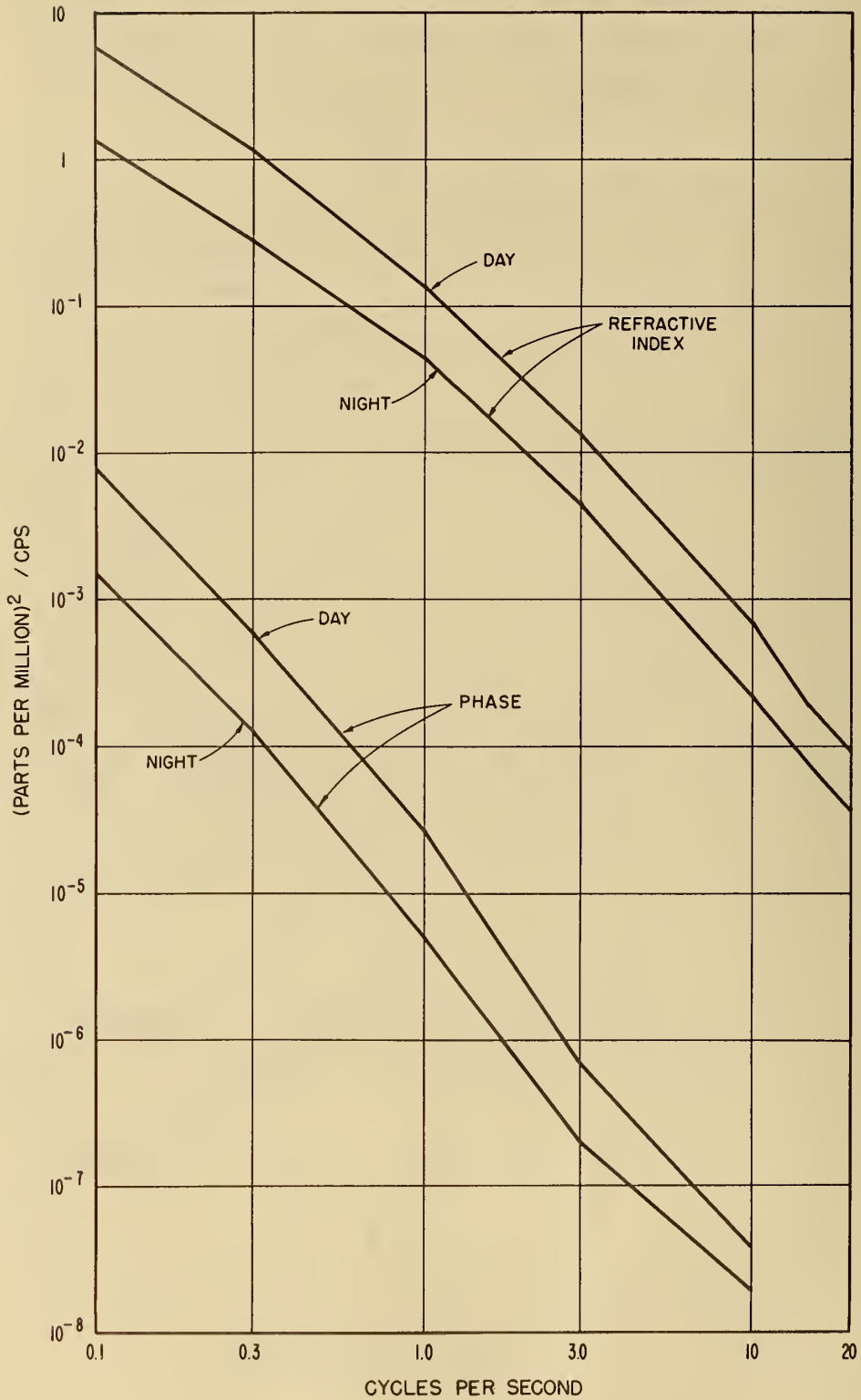


Figure 28

# APPARENT PATH LENGTH SPECTRAL DENSITY COMPARED WITH OTHER DATA

15.2 km (9.4 mi.) PATH, BOULDER, COLORADO

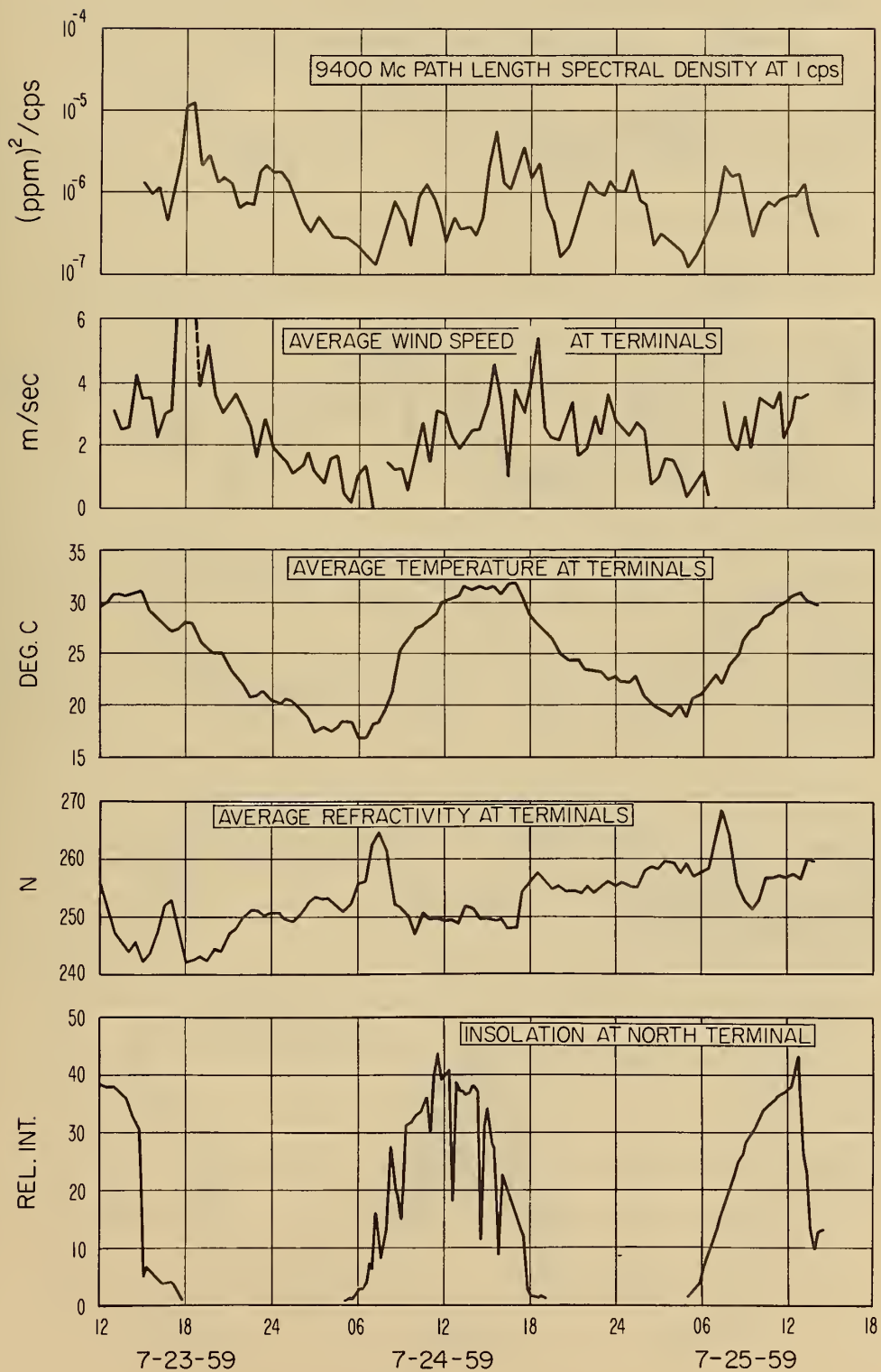


Figure 29

REFRACTIVITY SPECTRAL DENSITY COMPARED  
 WITH OTHER DATA TAKEN AT NORTH TERMINAL  
 15.2 km (9.4 mi.) PATH, BOULDER, COLORADO

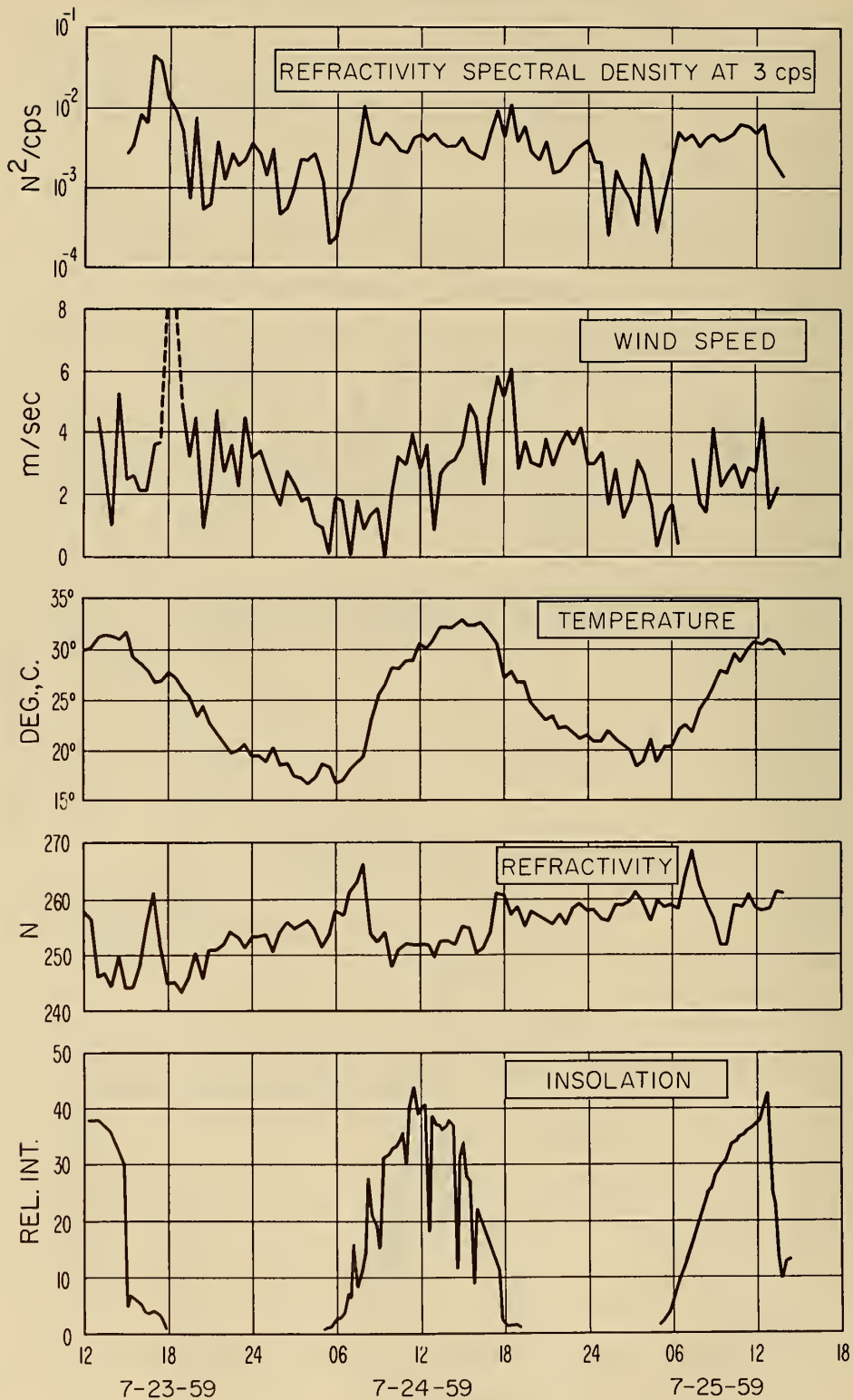


Figure 30



# REFRACTIVITY SPECTRAL DENSITY COMPARED WITH OTHER DATA TAKEN AT NORTH TERMINAL

7.7 km (4.8 mi.) PATH, CAPE CANAVERAL, FLORIDA

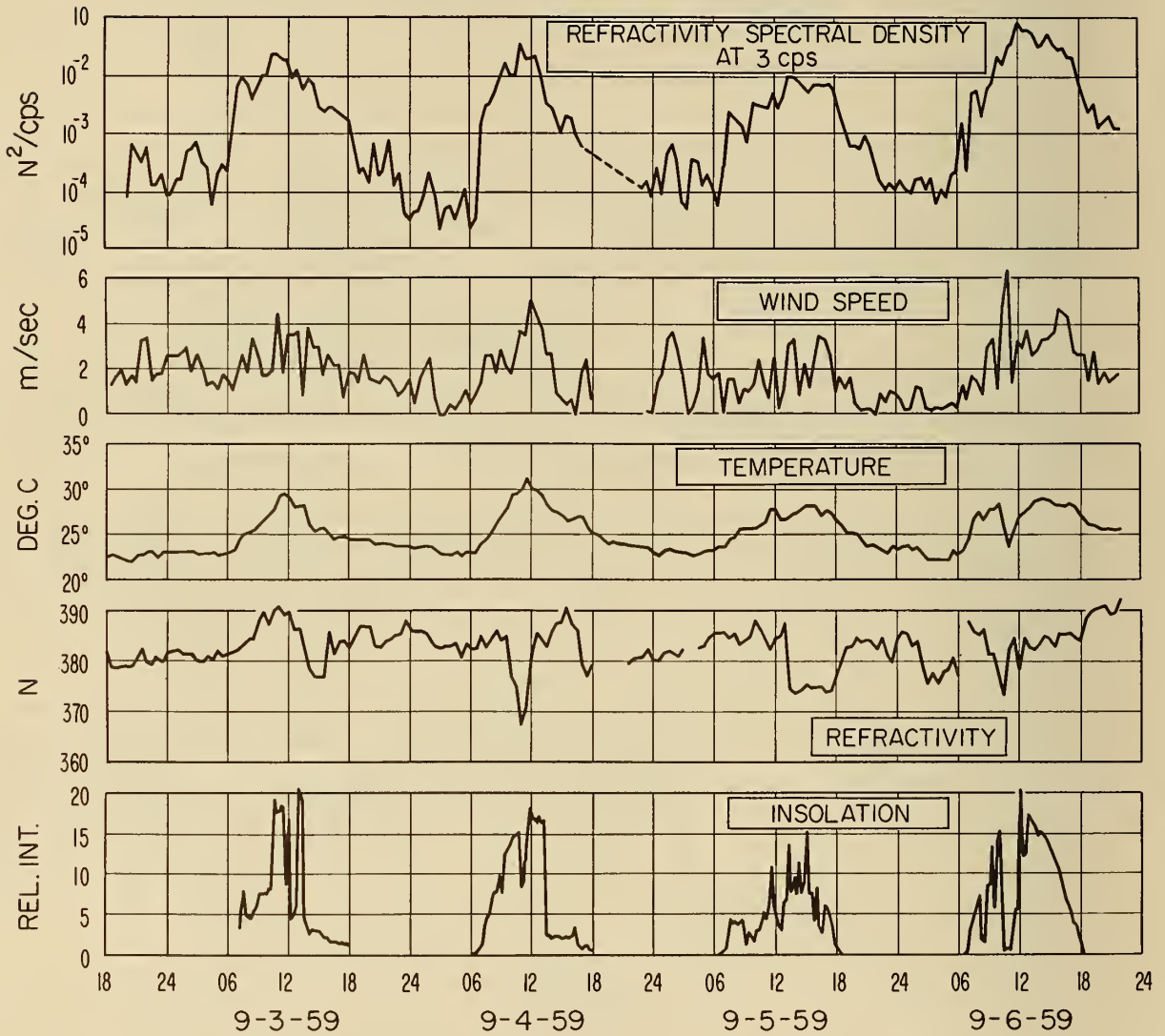


Figure 32

# APPARENT PATH LENGTH SPECTRAL DENSITY COMPARED WITH OTHER DATA

17.1 km (10.6mi.) PATH AT CAPE CANAVERAL, FLORIDA

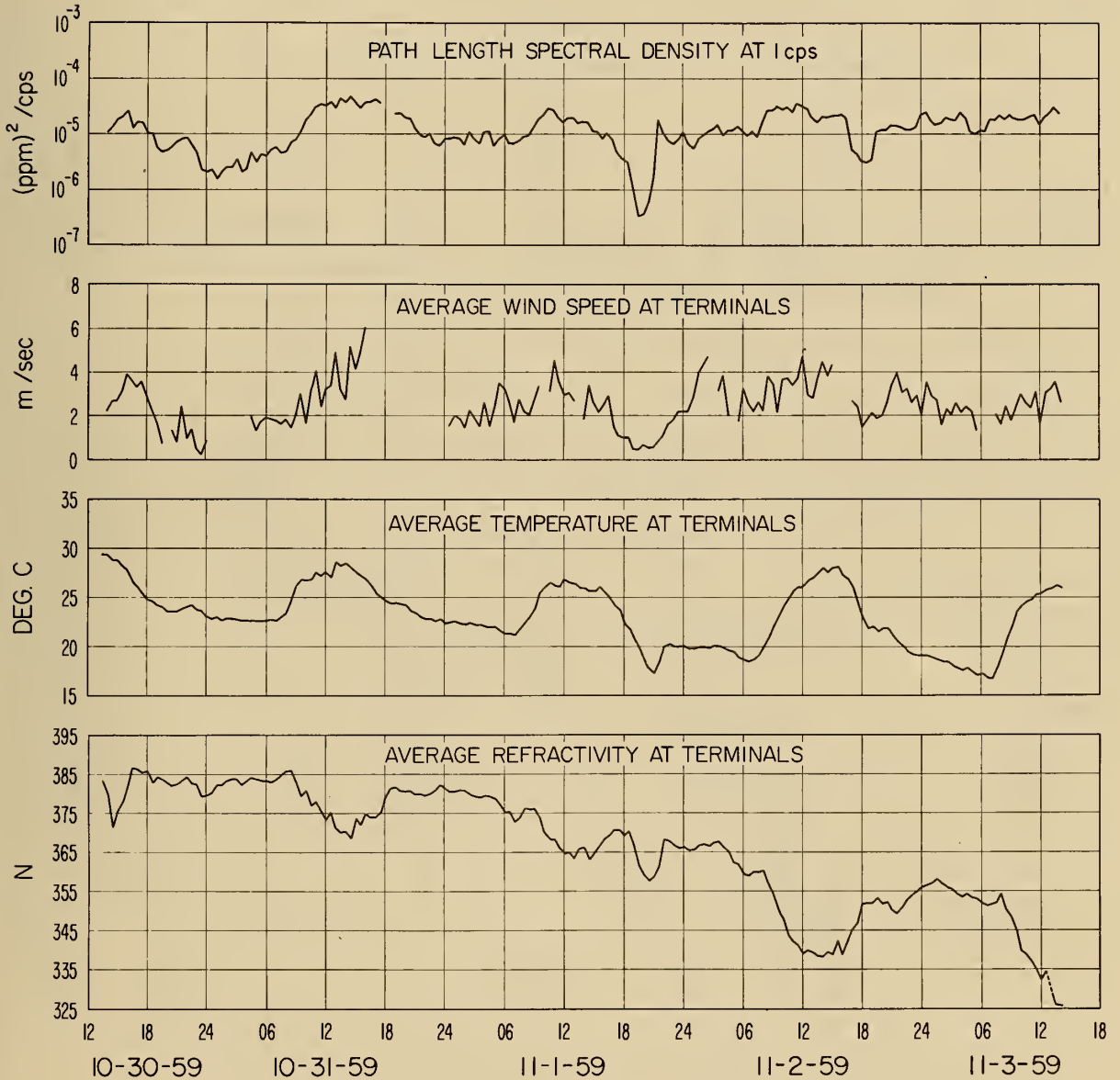


Figure 33



CORRELATION OF APPARENT PATH LENGTH SPECTRAL DENSITY WITH  
 AVERAGE END-POINT WIND SPEED AND TEMPERATURE

JULY 23-25, 1959

BOULDER, COLORADO

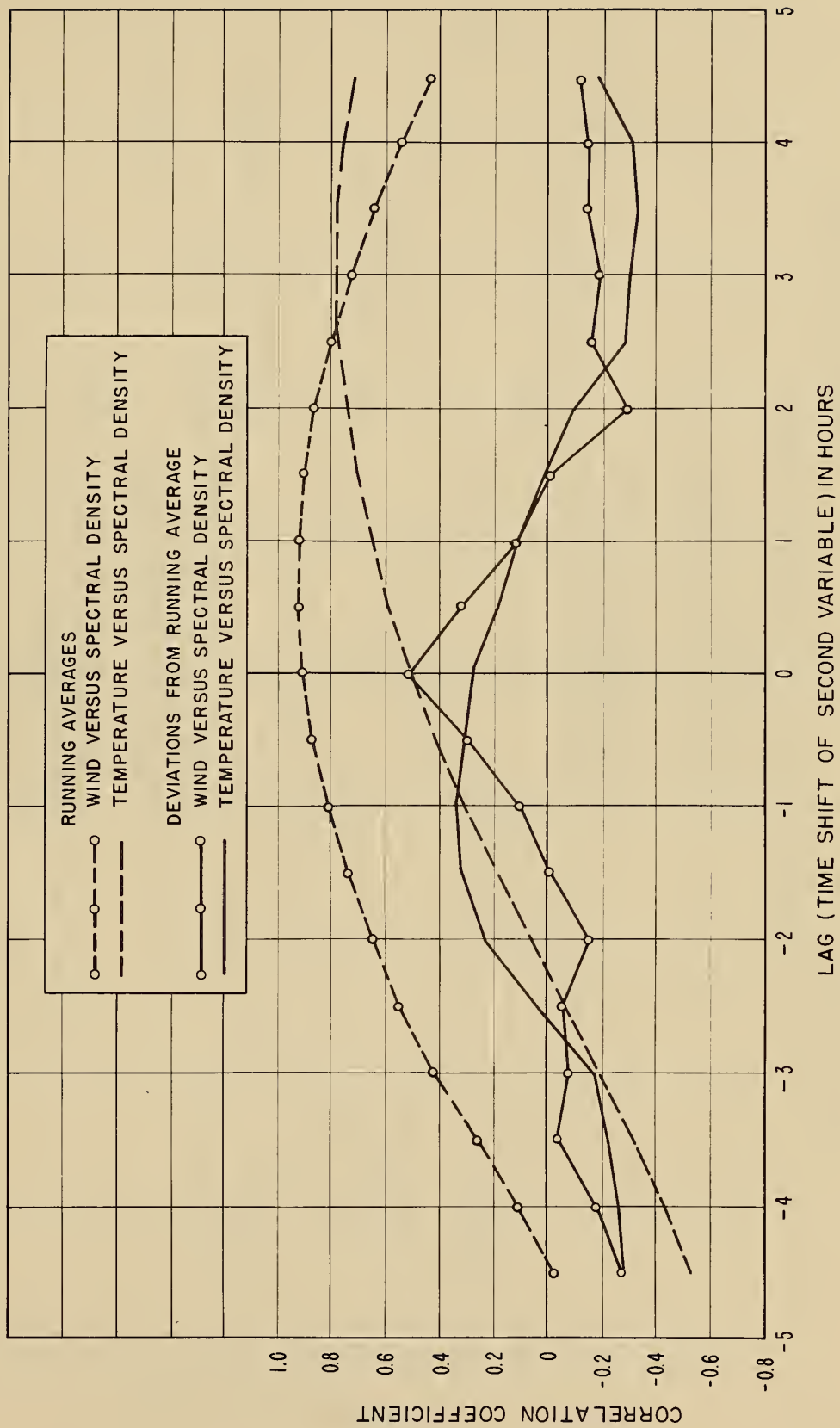


Figure 35

CORRELATION OF REFRACTIVITY SPECTRAL DENSITY WITH  
WIND SPEED AND TEMPERATURE

JULY 23 - 25, 1959

BOULDER, COLORADO

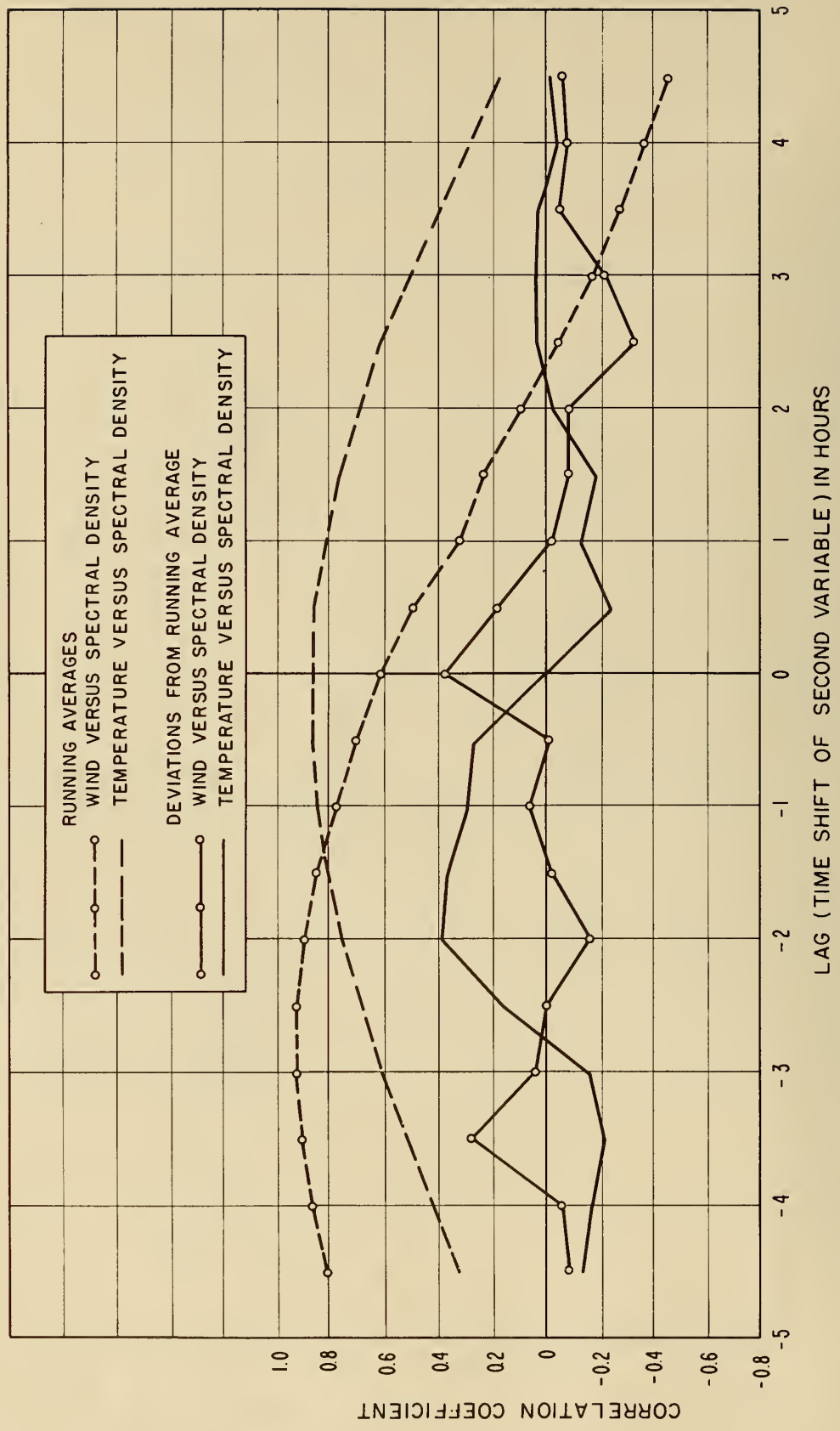


Figure 36

CORRELATION OF APPARENT PATH LENGTH SPECTRAL DENSITY WITH  
 AVERAGE END-POINT WIND SPEED AND TEMPERATURE

SEPTEMBER 2-4, 1959

CAPE CANAVERAL, FLORIDA

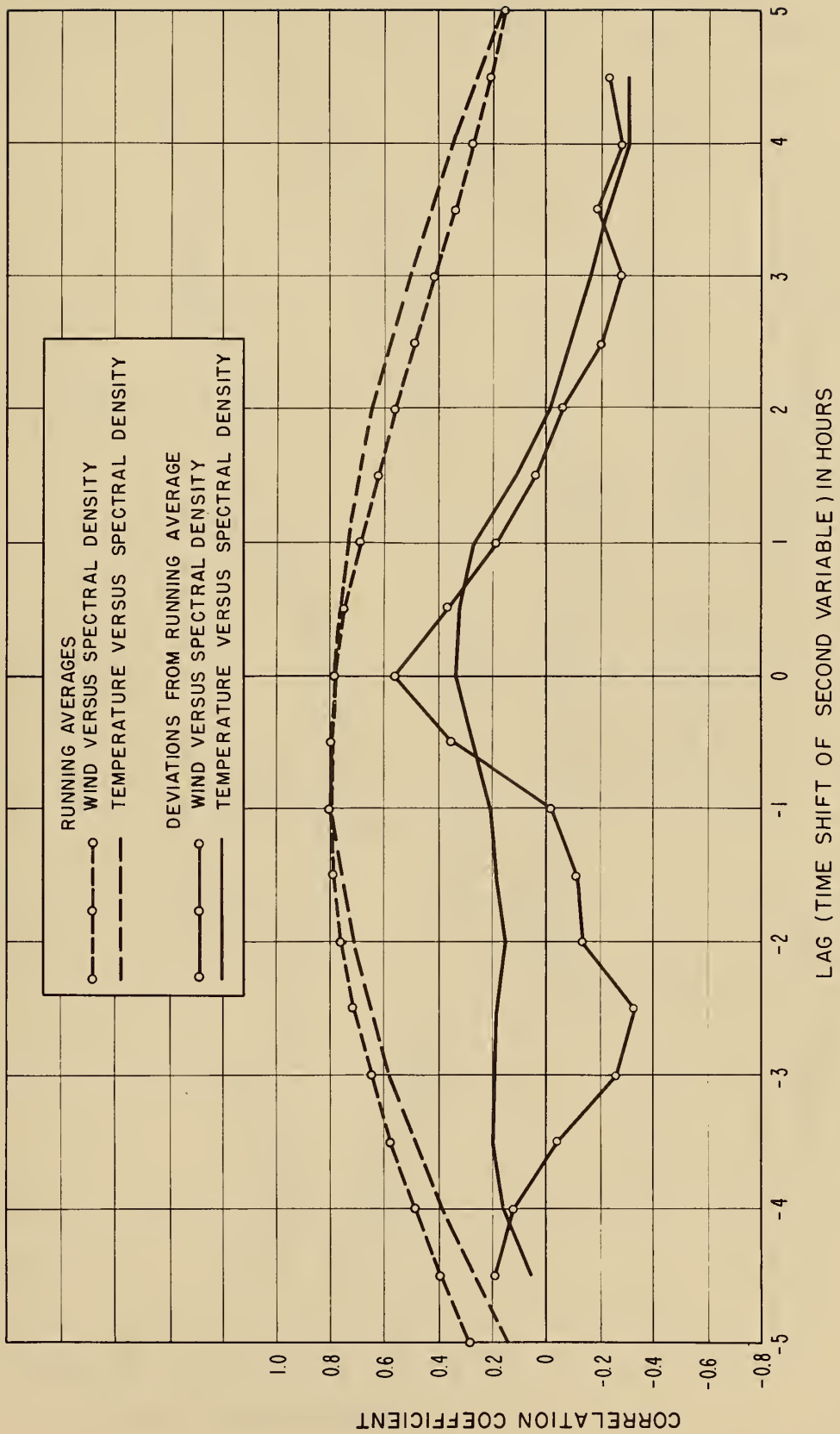


Figure 37

CORRELATION OF REFRACTIVITY SPECTRAL DENSITY WITH  
WIND SPEED AND TEMPERATURE

SEPTEMBER 2-4, 1959

CAPE CANAVERAL, FLORIDA

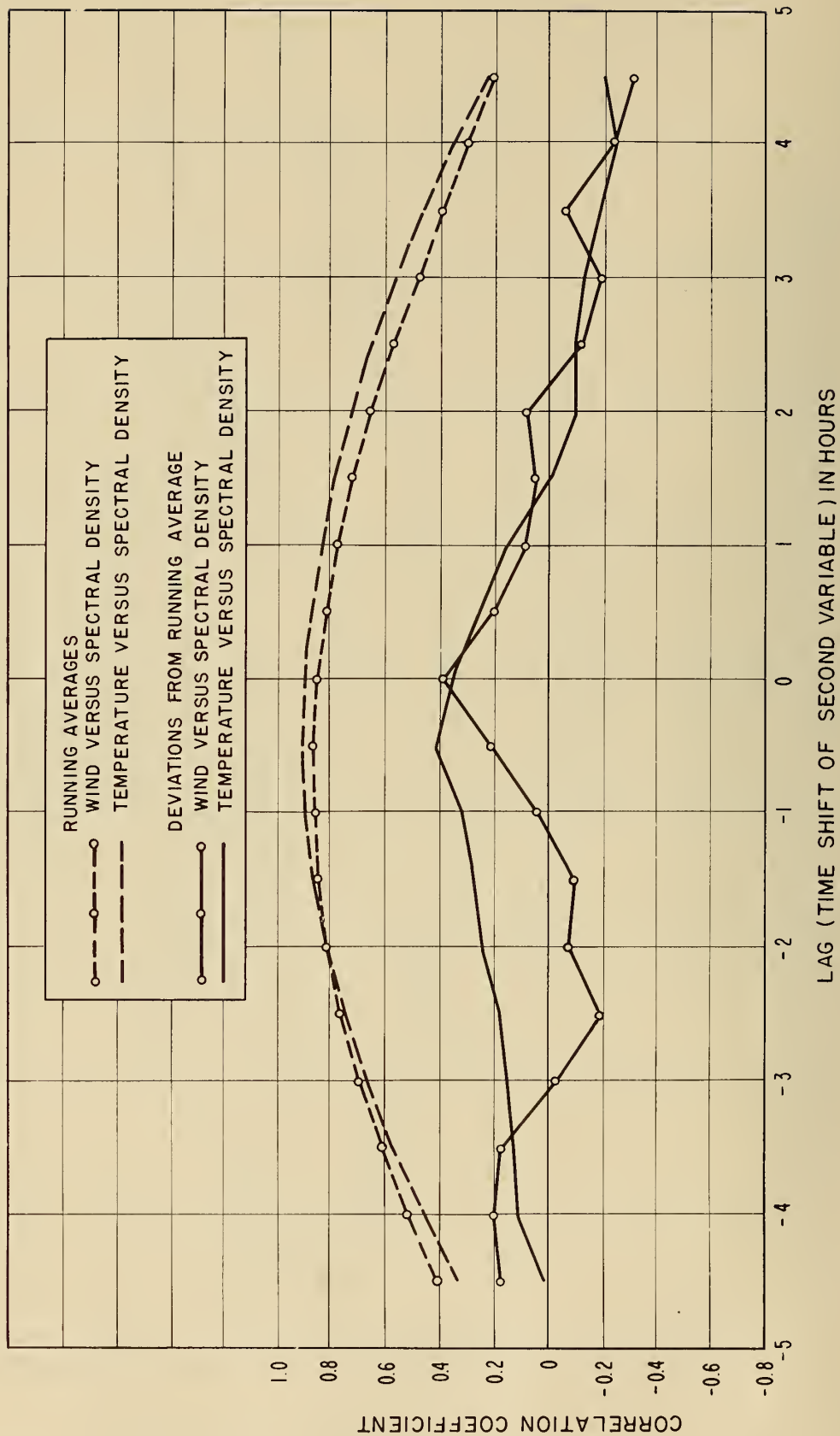


Figure 38

9400 Mc SIGNAL AMPLITUDE VARIATIONS  
7.7 km (4.8 mi.) PATH, CAPE CANAVERAL, FLA.—OCT. 1959

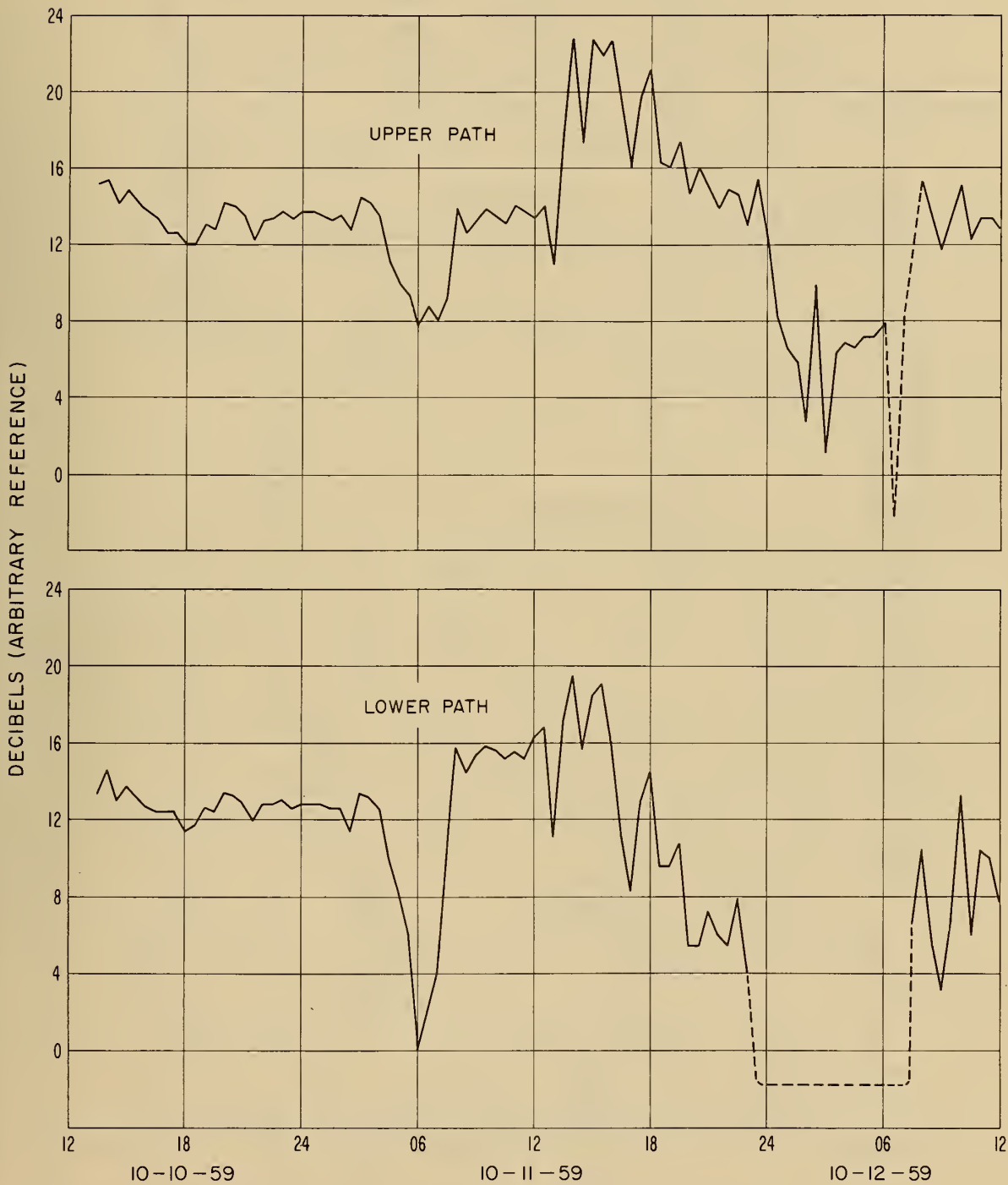


Figure 39

9400 MC SIGNAL AMPLITUDE VARIATIONS  
 17.1 km (10.6 mi.) PATH, CAPE CANAVERAL, FLORIDA, OCTOBER-NOVEMBER 1959

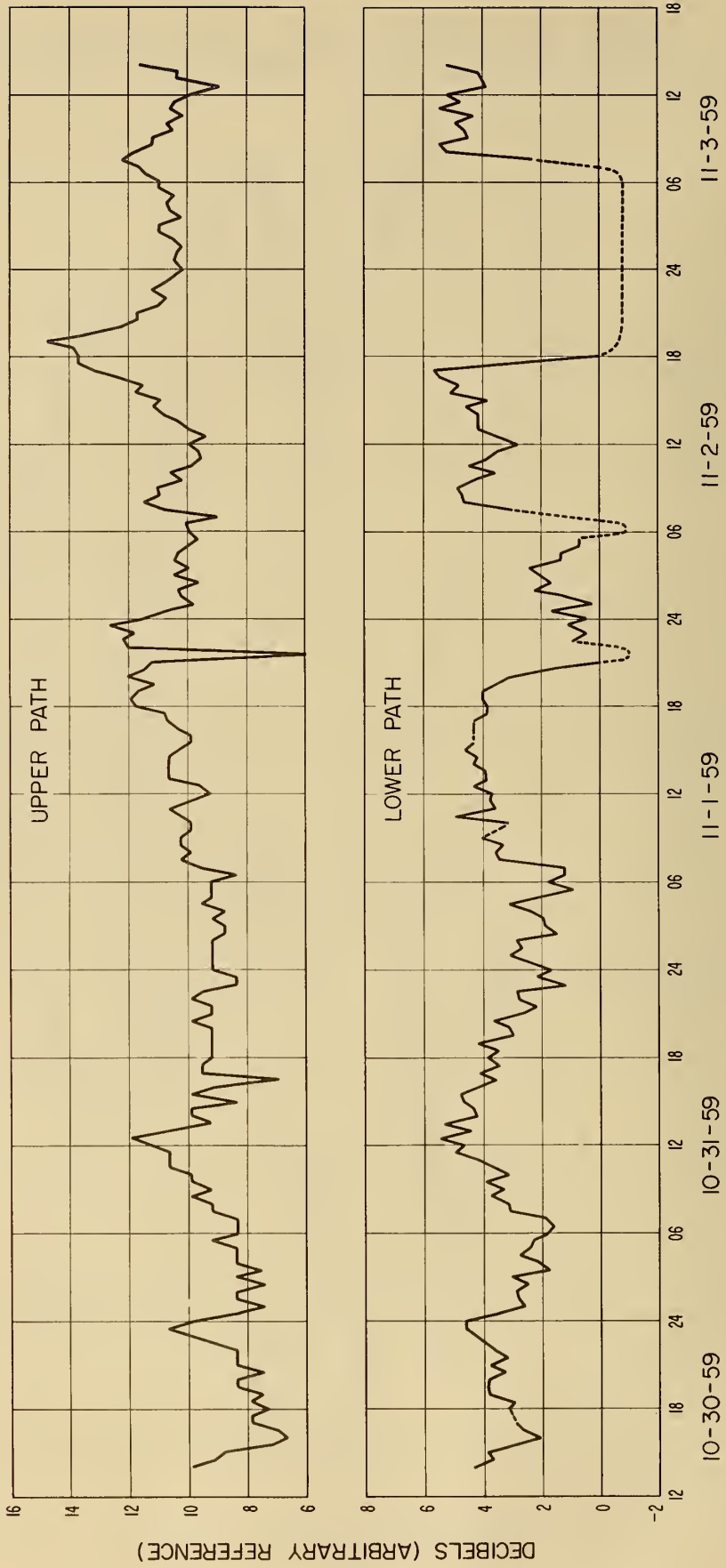


Figure 40

TIME VARIATIONS IN THE POWER SPECTRA  
 OF THE APPARENT PATH LENGTH OF 100 MC AND 9400 MC  
 15.2 km (9.4 mi.) PATH AT BOULDER, COLORADO

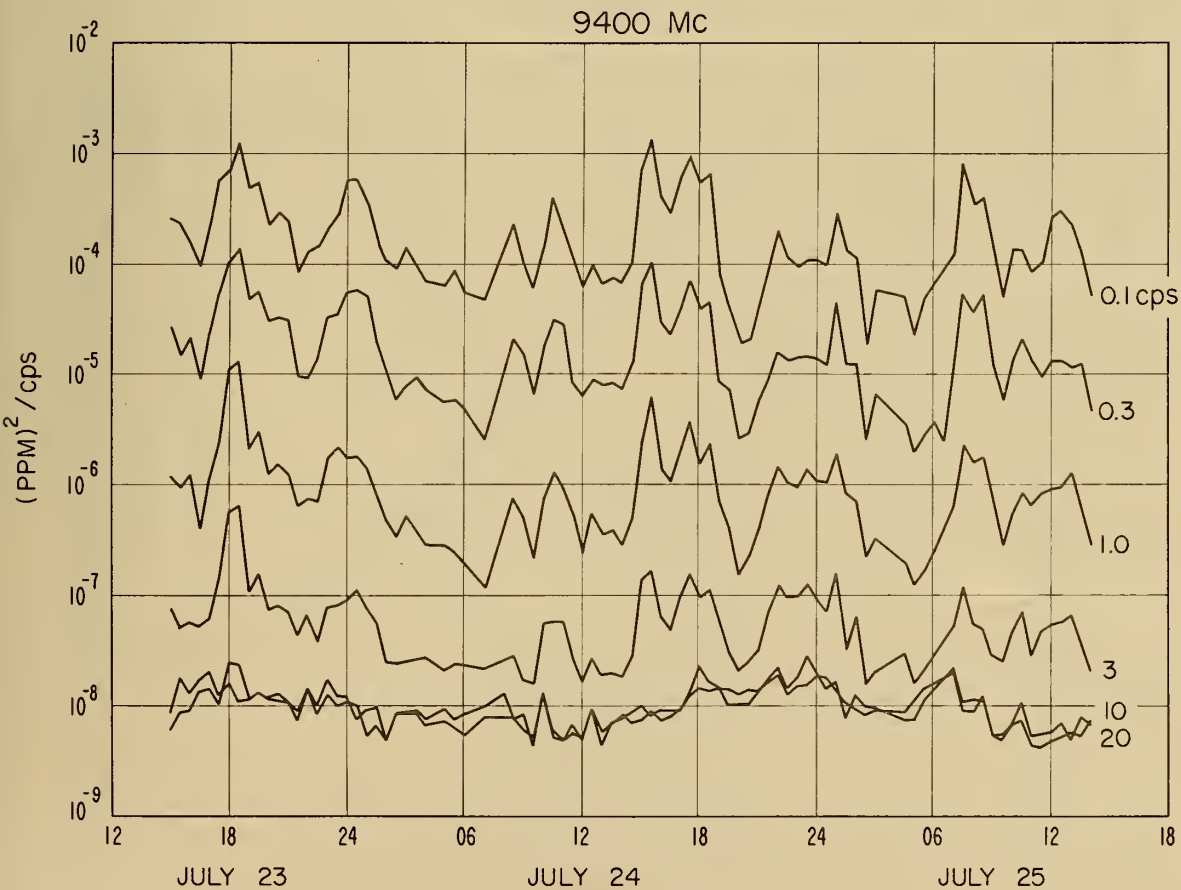
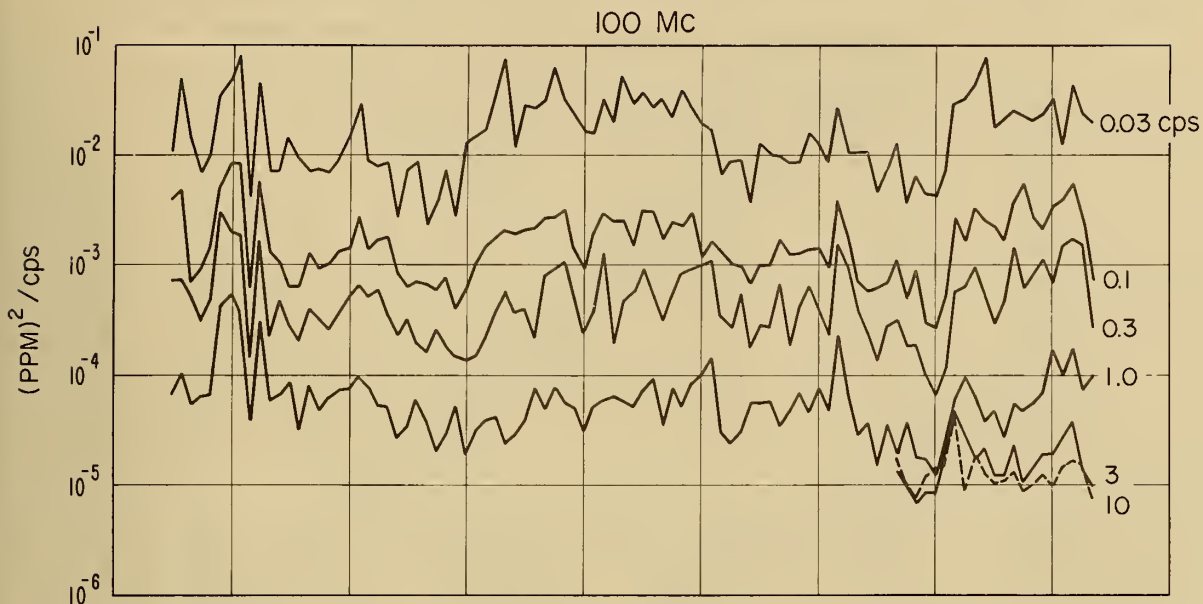


Figure 41

COMPARISON OF 100 Mc AND 9400 Mc SPECTRA  
OBSERVED IN BOULDER, COLORADO

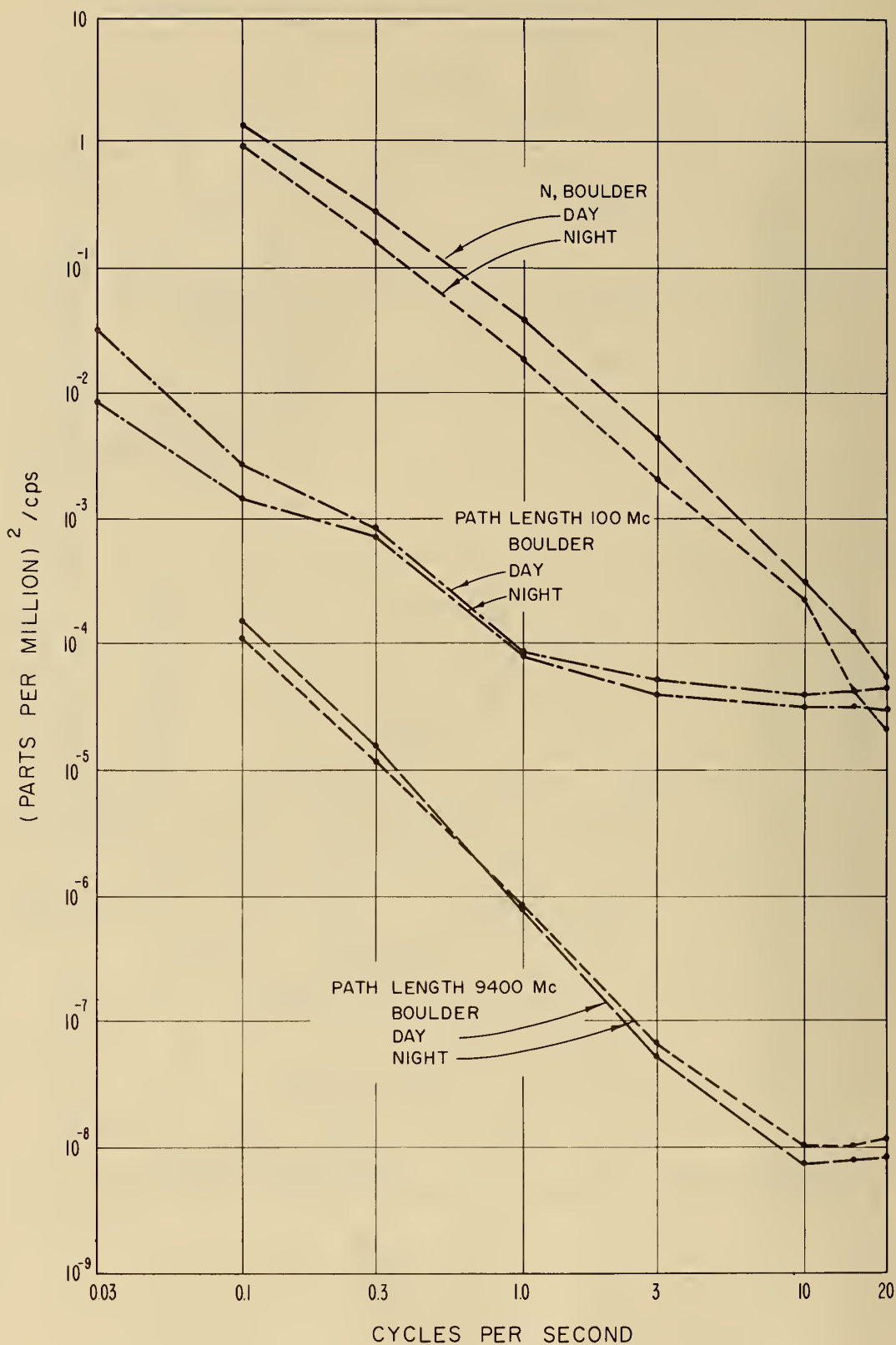


Figure 42



TIME VARIATIONS IN THE POWER SPECTRUM OF  
 APPARENT LENGTH OF LOWER PATH

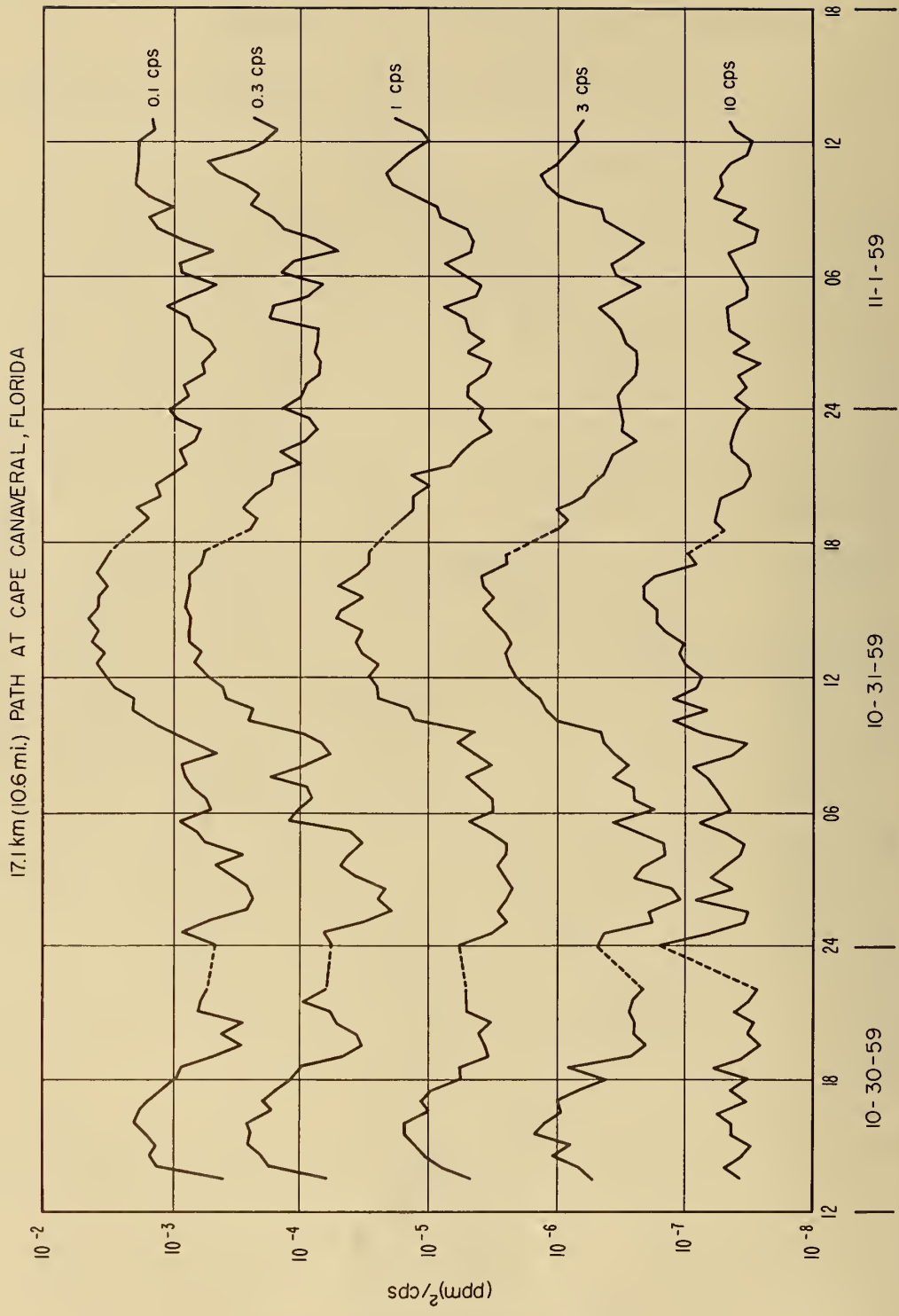


Figure 44

MEDIAN POWER SPECTRA OF PATH LENGTH VARIATIONS  
ON TWO VERTICALLY-SEPARATED PATHS

17.1 km. (10.6 MI.) PATHS AT CAPE CANAVERAL, FLORIDA

OCT. 30 - NOV. 1, 1959

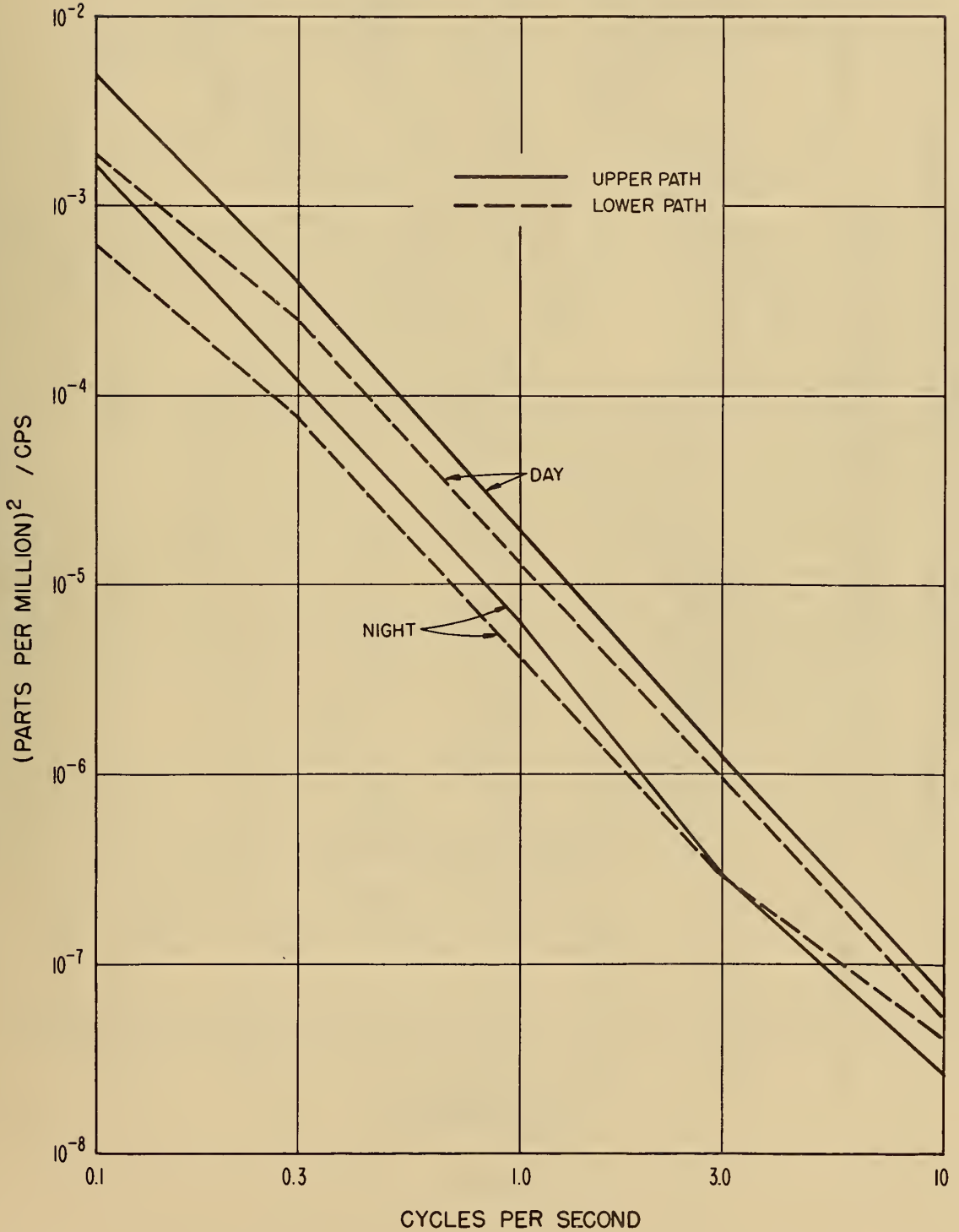


Figure 45

TIME VARIATIONS IN THE POWER SPECTRUM OF  
 APPARENT ELEVATION ANGLE (PATH DIFFERENCE) VARIATIONS

17.1 km (10.6 mi) PATH AT CAPE CANAVERAL, FLORIDA

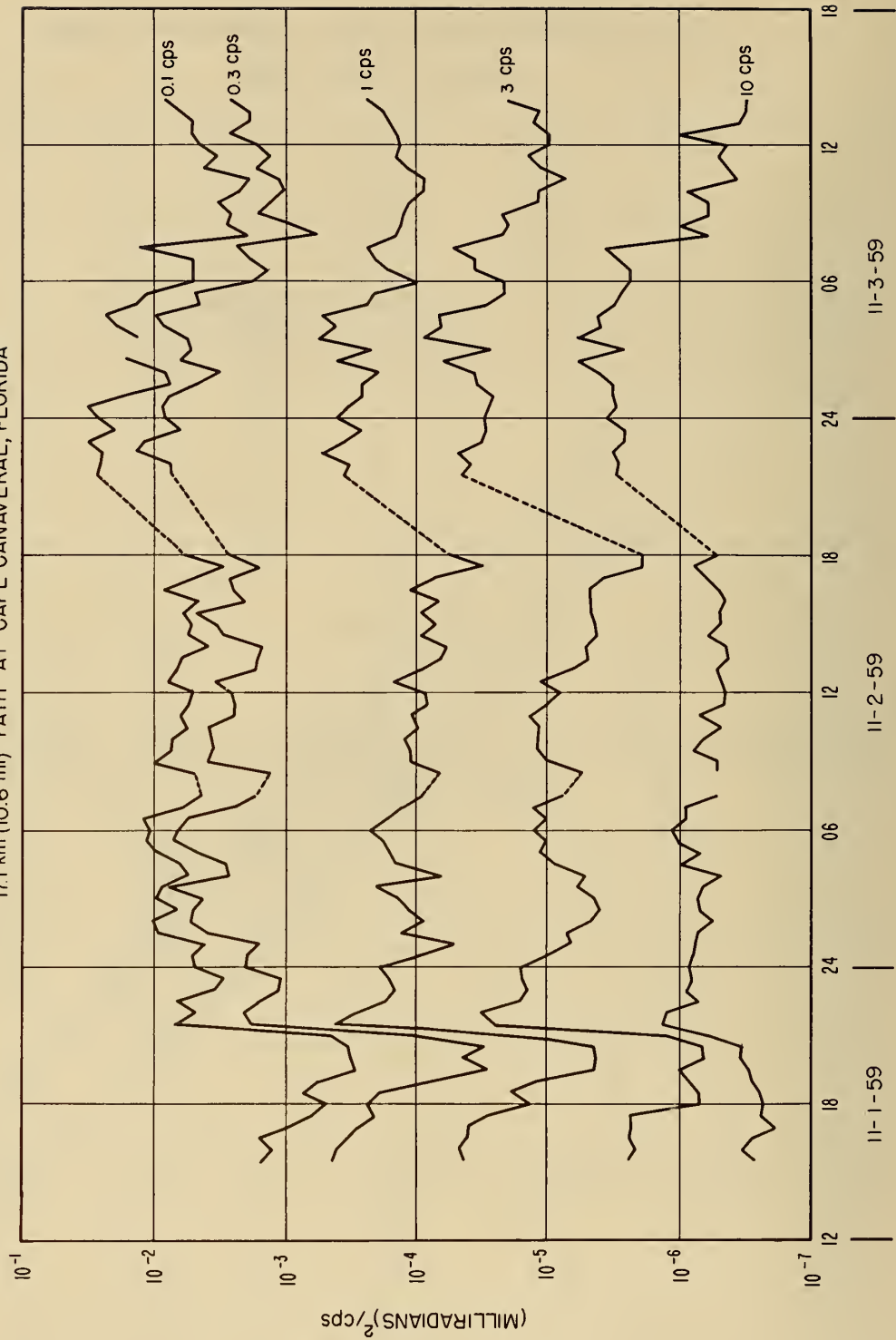


Figure 46

MEDIAN POWER SPECTRA OF APPARENT ELEVATION ANGLE (PATH DIFFERENCE)  
VARIATIONS 17.1 km. (10.6 MI.) PATH AT CAPE CANAVERAL, FLA.

NOVEMBER 1-3, 1959

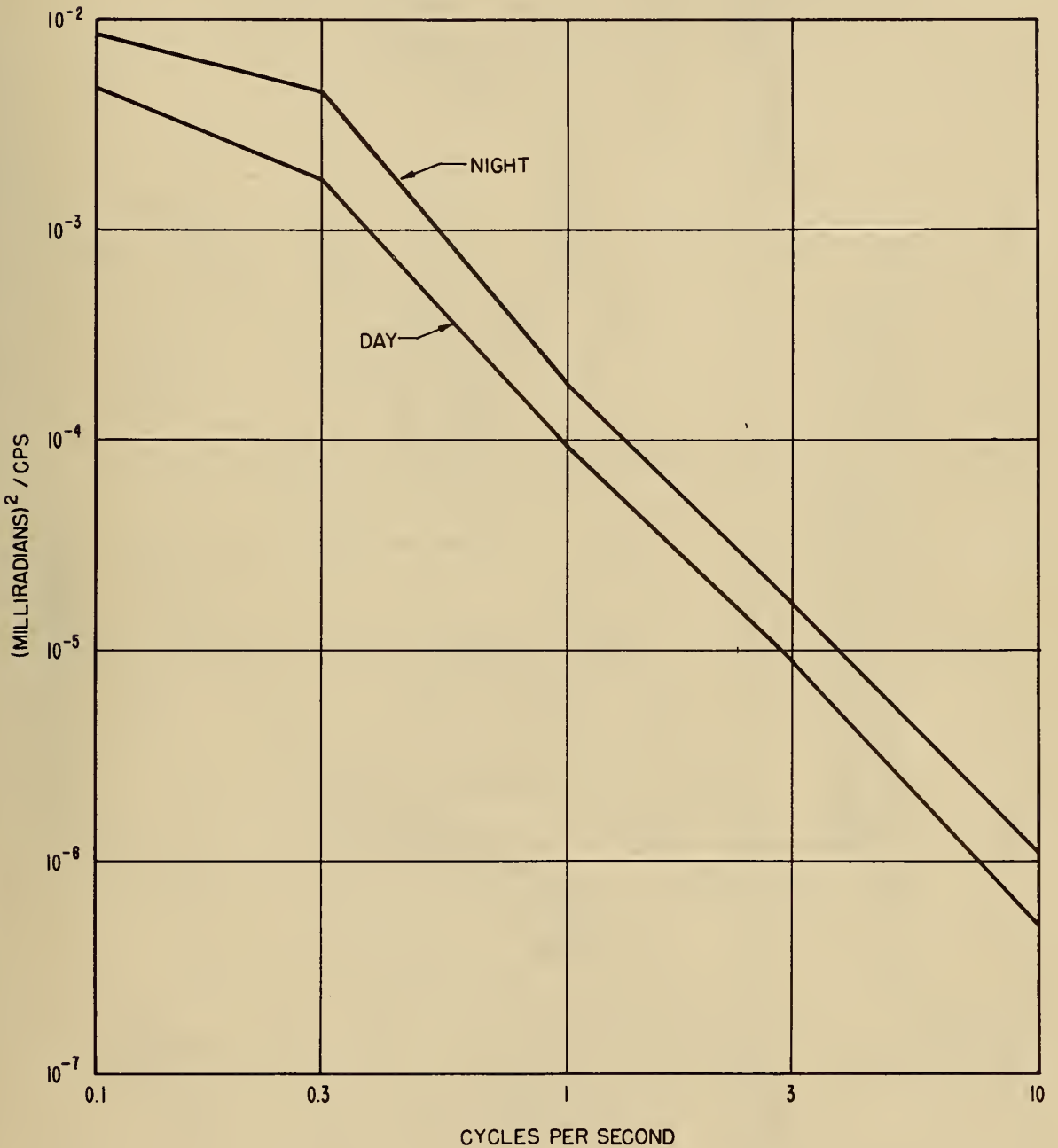


Figure 47

TIME VARIATIONS IN THE POWER SPECTRUM OF  
 APPARENT LENGTH OF SHORT (30 m) PATH

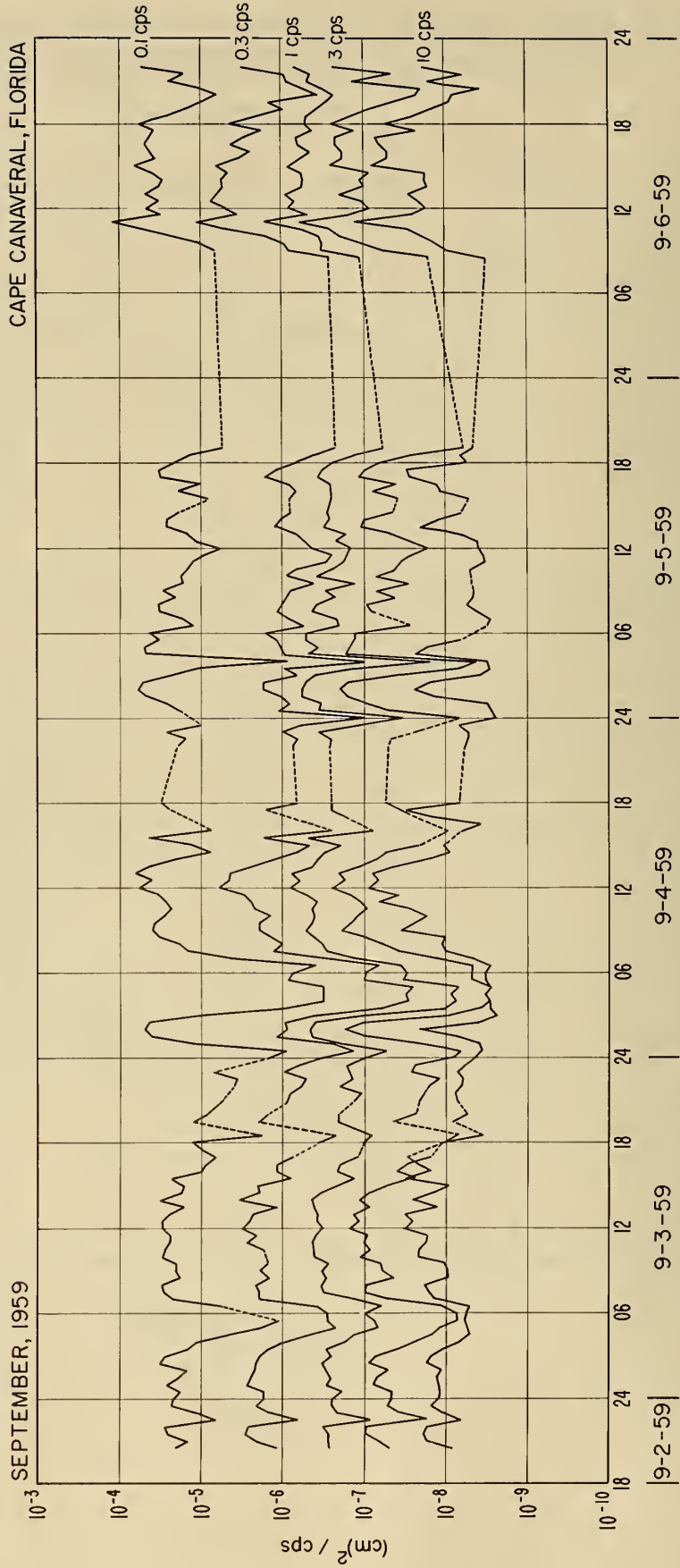


Figure 48

MEDIAN POWER SPECTRA OF APPARENT PATH LENGTH VARIATIONS  
ON LONG AND SHORT PATHS

SEPTEMBER 1959

CAPE CANAVERAL, FLORIDA

(ORDINATE REFERS TO PARTS PER MILLION ON LONG PATH)

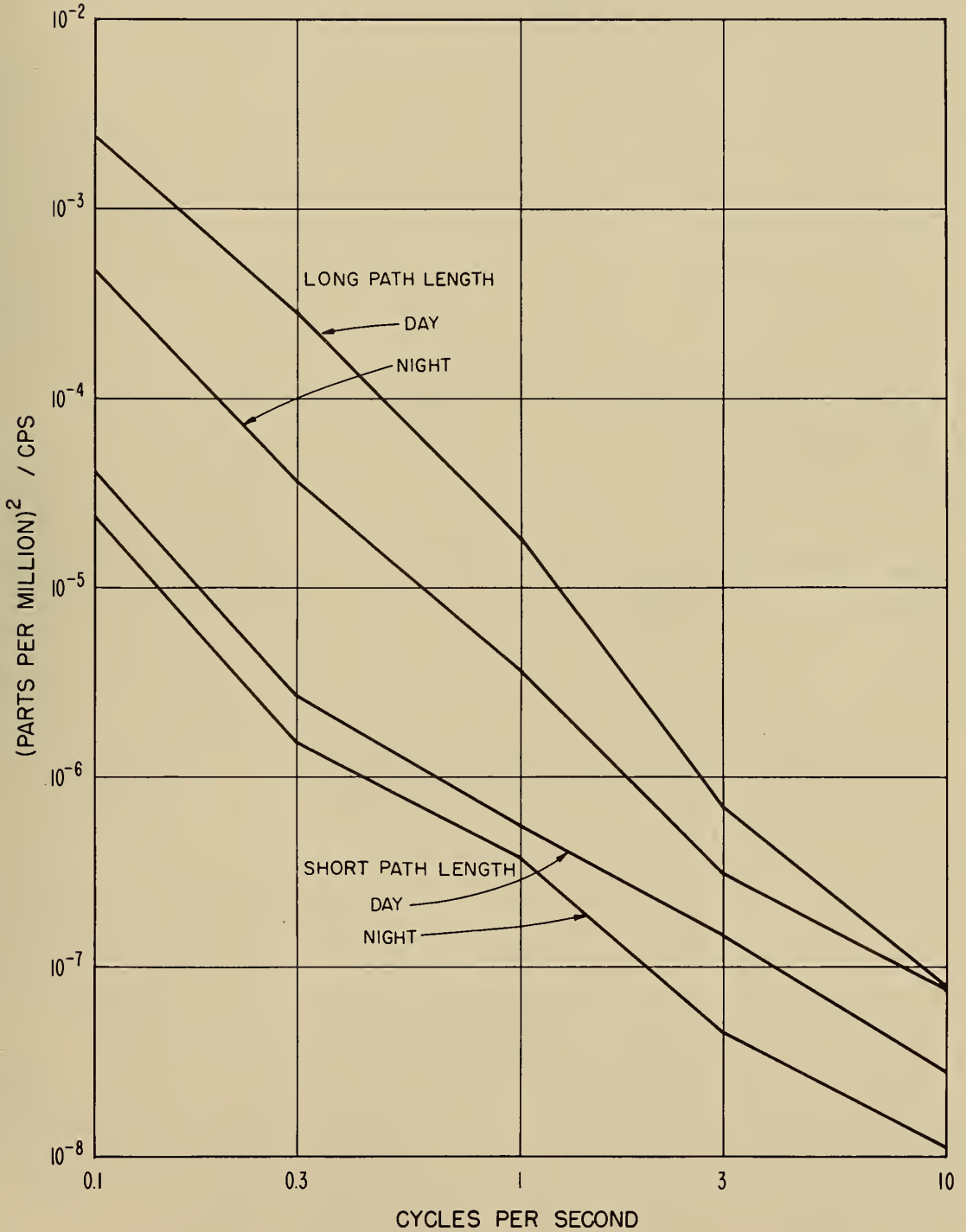


Figure 49

AIR TEMPERATURE AND REFRACTIVITY COMPARED TO  
APPARENT PATH LENGTH VARIATIONS ON SHORT (30 m) PATH

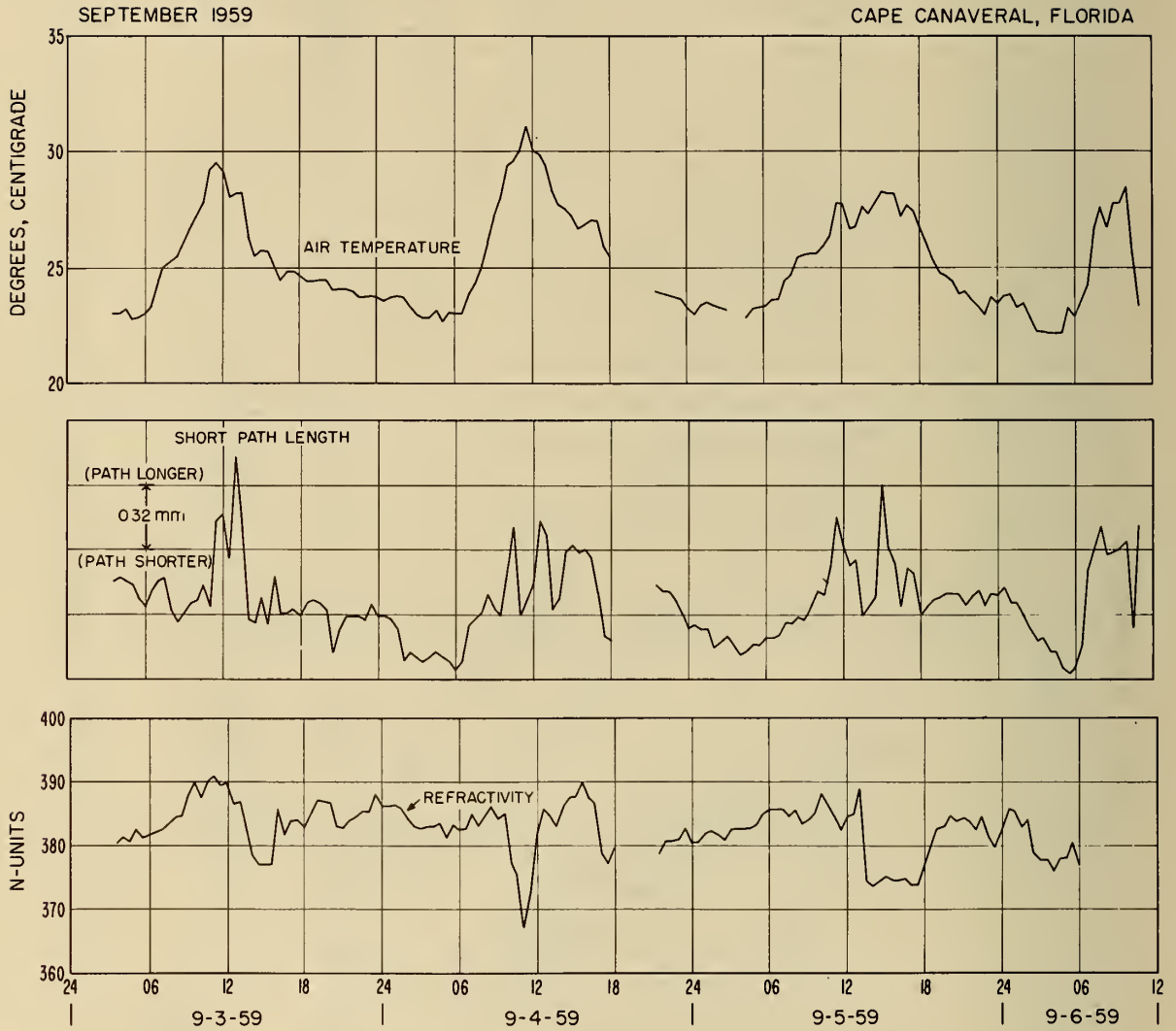


Figure 50















